Study of Detection Performance of Silicon Strip Sensors for ATLAS ITk Upgrade Project

Věra Latoňová

Supervisor: Ing. Marcela Mikeštíková, Ph.D.

Consultant: doc. RNDr. Zdeněk Doležal, Dr.

7th April 2018

- one of the major experiments at LHC
- cylinder - $l = 46\,\mathrm{m}$, $d = 25\,\mathrm{m}$, $m = 7{,}000$ tonnes
- 6 different detecting subsystems $\rightarrow$ energy, momentum, trajectory of particles
- investigates broad range of physics: Standard Model, antimatter, dark matter ...
- discovery of Higgs boson $\rightarrow$ search for new physics

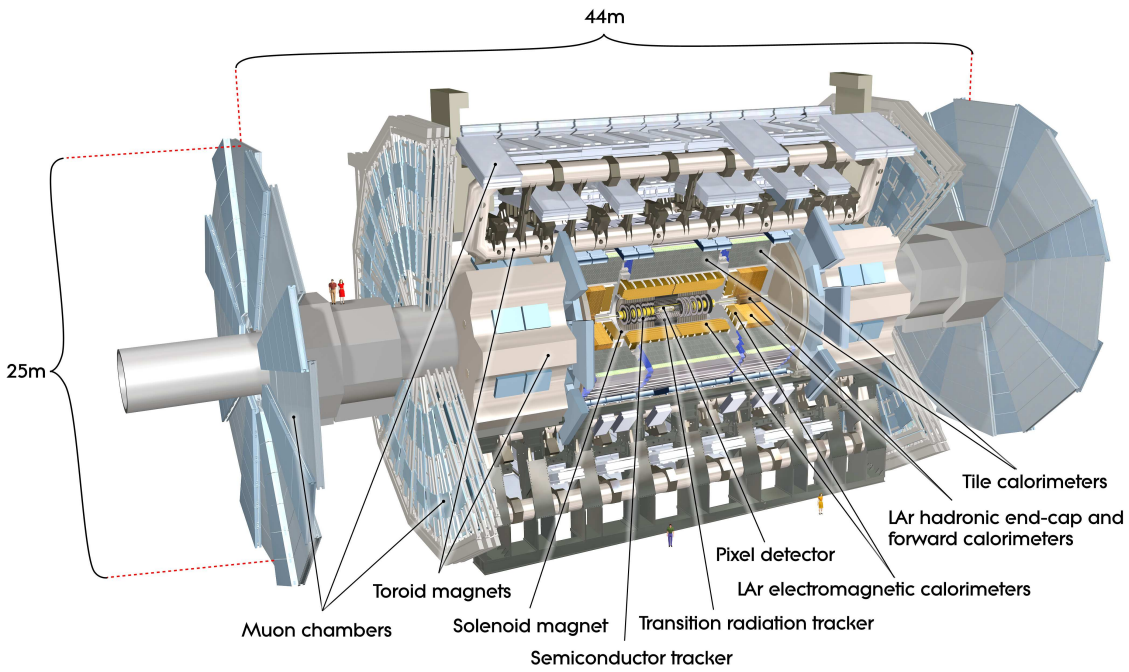

ATLAS Inner Detector (ID)

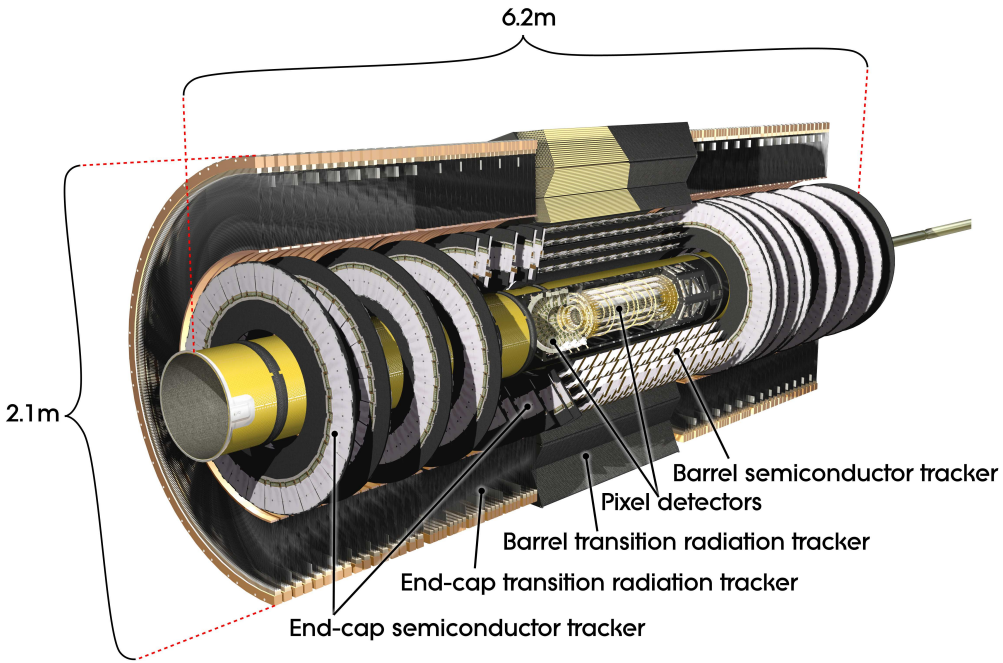

- Measures direction, momentum and charge
- Three sub-systems
  - Pixel detector
  - SemiConductor Tracker (SCT)
  - Transition Radiation Tracker (TRT)
- Designed for:
  - peak $L = 10^{34}\,\mathrm{cm}^{-2}\mathrm{s}^{-1}$
  - 27 pile-up events per 25 ns bunch crossing
  - level-1 trigger rate of 100 kHz

Motivation for the upgrade (ID $\rightarrow$ ITk)

- LHC $\rightarrow$ HL-LHC (2024)
- Occupancy
- Bandwidth saturation
- Radiation damage

	ID	Phase I	Phase II
$L[10^{34}\mathrm{cm}^{-2}\mathrm{s}^{-1}]$	1	2.2	5-7
$L_{\mathrm{int}}[\mathrm{fb}^{-1}]$	75	300-400	3000
μ	27	55	140-200

Motivation for the upgrade (ID $\rightarrow$ ITk)

- LHC $\rightarrow$ HL-LHC (2024)
- Occupancy
- Bandwidth saturation
- Radiation damage

	ID	Phase I	Phase II
$L[10^{34}\mathrm{cm}^{-2}\mathrm{s}^{-1}]$	1	2.2	5-7
$L_{\mathrm{int}}[\mathrm{fb}^{-1}]$	75	300-400	3000
μ	27	55	140-200

Intrinsic semiconductors

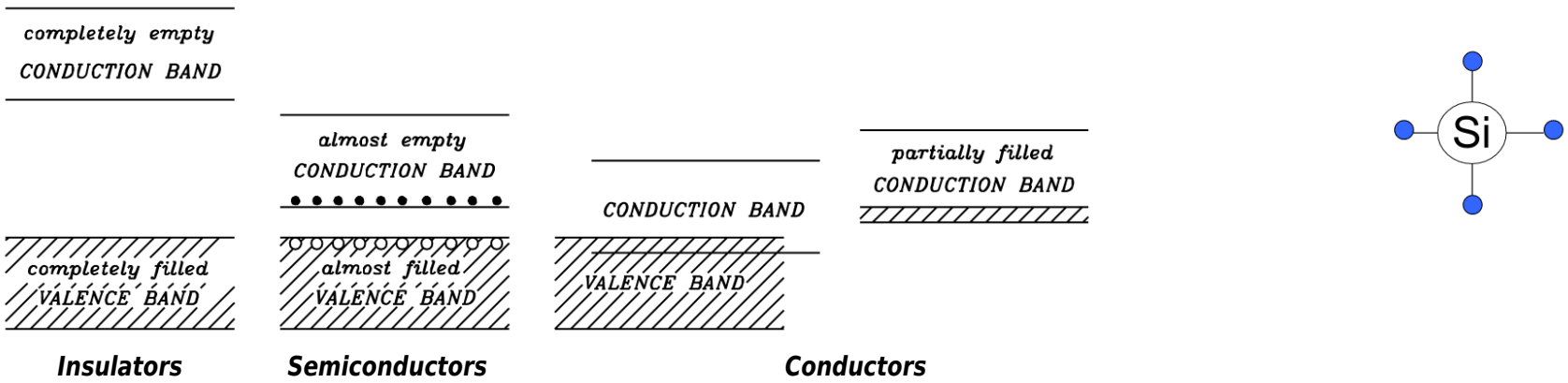

- Semiconductors made from atoms of the same species
- Si, Ge, GaAs
- Narrow energy gap ($\sim 1\,\mathrm{eV}$)
- Conductivity by thermally excited electrons
- Carrier concentration in pure silicon is $\sim (10^{10} - 10^{11})\,\mathrm{cm}^{-3}$ at 300 K - too low for a simple crystal detector

Extrinsic semiconductors and p-n junction

- Carrier concentration can be influenced by doping → extrinsic semiconductors
  - n-type semiconductors
  - p-type semiconductors
- PN-junction
  - diffusion until equilibrum
  - potential barrier → deplation layer
  - increase of the depletion width by applying negative voltage – reverse bias

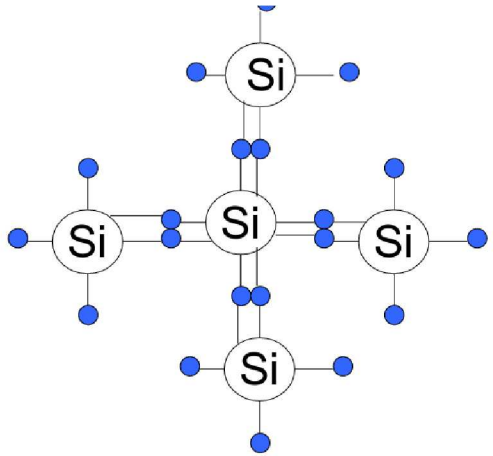

Extrinsic semiconductors and p-n junction

- Carrier concentration can be influenced by doping → extrinsic semiconductors
  - n-type semiconductors
  - p-type semiconductors
- PN-junction
  - diffusion until equilibrum
  - potential barrier → deplation layer
  - increase of the depletion width by applying negative voltage – reverse bias

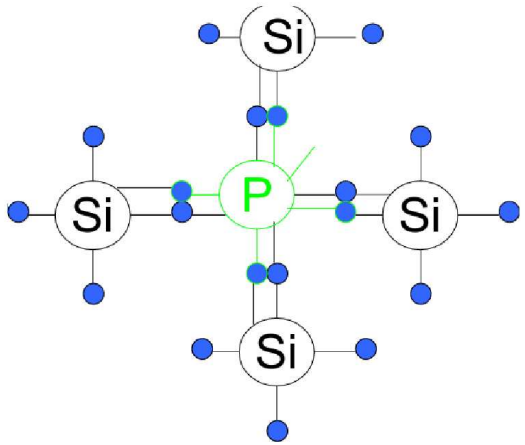

Extrinsic semiconductors and p-n junction

- Carrier concentration can be influenced by doping → extrinsic semiconductors
  - n-type semiconductors
  - p-type semiconductors
- PN-junction
  - diffusion until equilibrum
  - potential barrier → deplation layer
  - increase of the depletion width by applying negative voltage – reverse bias

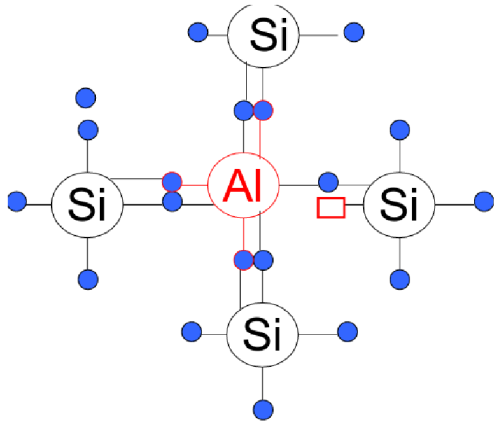

Extrinsic semiconductors and p-n junction

- Carrier concentration can be influenced by doping → extrinsic semiconductors
  - n-type semiconductors
  - p-type semiconductors
- PN-junction
  - diffusion until equilibrum
  - potential barrier → deplation layer
  - increase of the depletion width by applying negative voltage – reverse bias

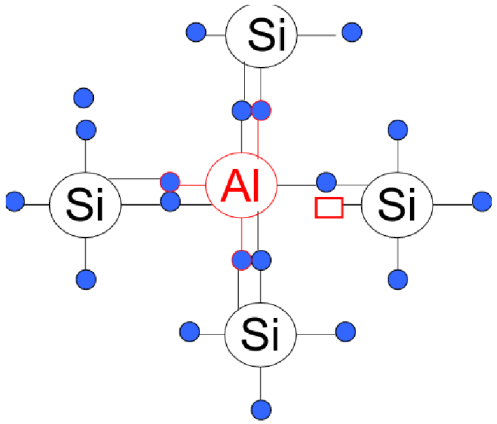

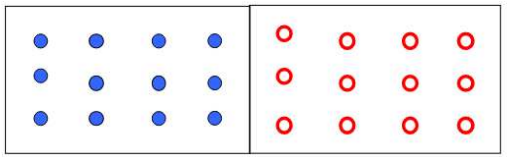

Extrinsic semiconductors and p-n junction

- Carrier concentration can be influenced by doping → extrinsic semiconductors
  - n-type semiconductors
  - p-type semiconductors
- PN-junction
  - diffusion until equilibrum
  - potential barrier → deplation layer
  - increase of the depletion width by applying negative voltage – reverse bias

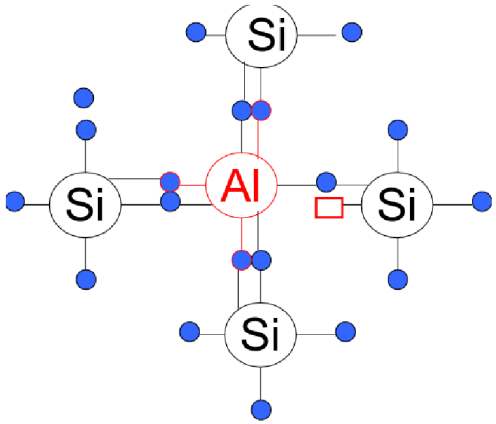

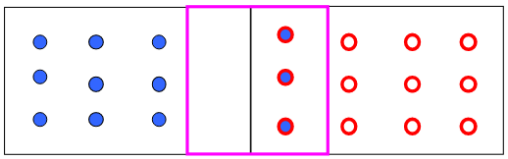

Extrinsic semiconductors and p-n junction

- Carrier concentration can be influenced by doping → extrinsic semiconductors
  - n-type semiconductors
  - p-type semiconductors
- PN-junction
  - diffusion until equilibrum
  - potential barrier → deplation layer
  - increase of the depletion width by applying negative voltage – reverse bias

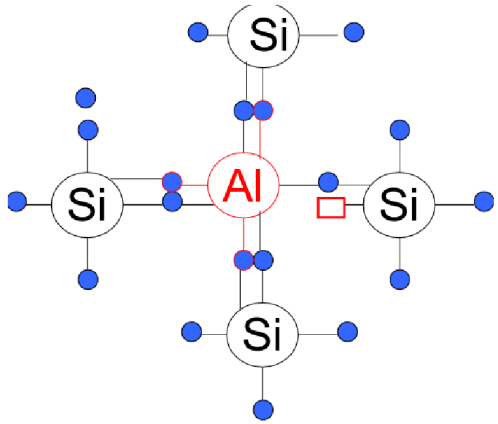

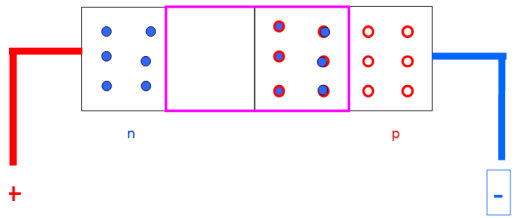

Principles of detection in silicon detectors

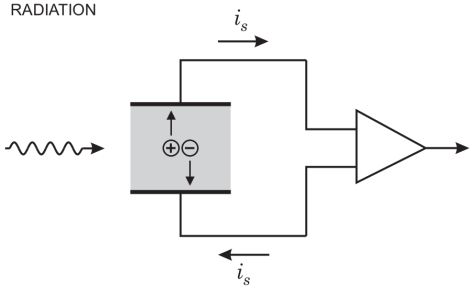

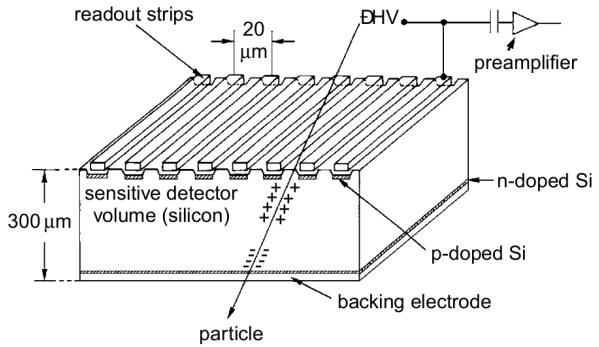

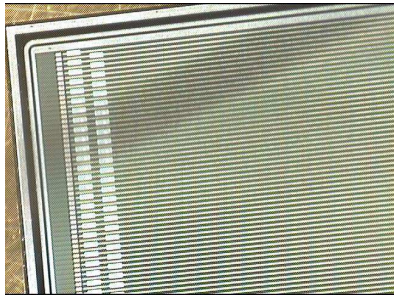

- Particles pass through detector → e-h pairs → electrodes
- Improvement of spatial resolution by segmenting the electrodes (pads/strips)
- Each strip is a pn-diode

Why silicon

- Low ionization energy ≈ 3.6 eV
- Long mean free path ≈ 100 nm
- Large energy loss per distance ≈ 3.8 MeV/cm (MIP)
- High carrier mobility at room temperature
- Possible electronics integration

Principles of detection in silicon detectors

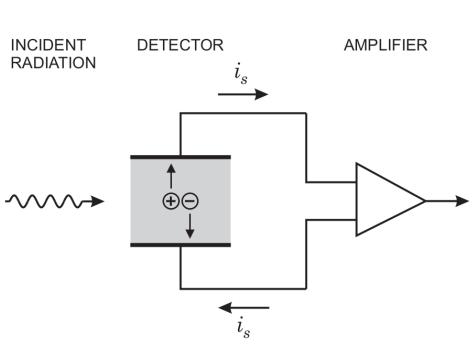

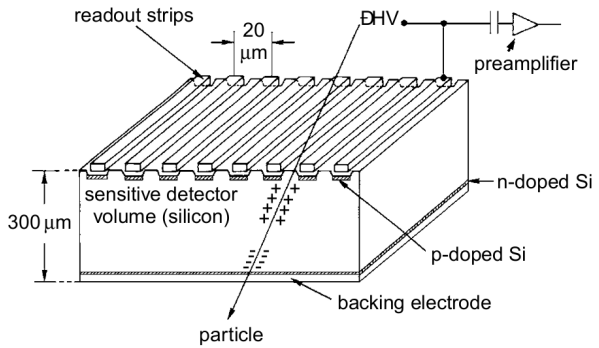

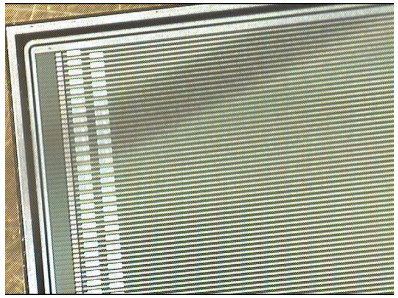

- Particles pass through detector $\rightarrow$ e-h pairs $\rightarrow$ electrodes
- Improvement of spatial resolution by segmenting the electrodes (pads/strips)
- Each strip is a pn-diode

Why silicon

- Low ionization energy $\approx 3.6\,\text{eV}$
- Long mean free path $\approx 100\,\text{nm}$
- Large energy loss per distance $\approx 3.8\,\text{MeV/cm}$ (MIP)
- High carrier mobility at room temperature
- Possible electronics integration

Radiation damage

- Bulk damage – primary caused by displacements of silicon atoms from their lattice sites
  - Depends on the energy and momentum transfer to the lattice atoms
  - conveniently measured in NIEL (non-ionizing energy loss)
  - Vacancies, interstitials, clusters

  → Increase of detector operating voltage

  → Increase of reverse-bias current in the space-charge region
  - Annealing
- Surface damage - effects in the SiO_2 layers and interface regions primary caused by ionization
  - Independent on the particle type
  - Proportional to the absorbed energy per unit volume - measured in in rad or gray of a specific absorber

  → Free charge carriers in the region

  → Parasitic fields

Radiation damage

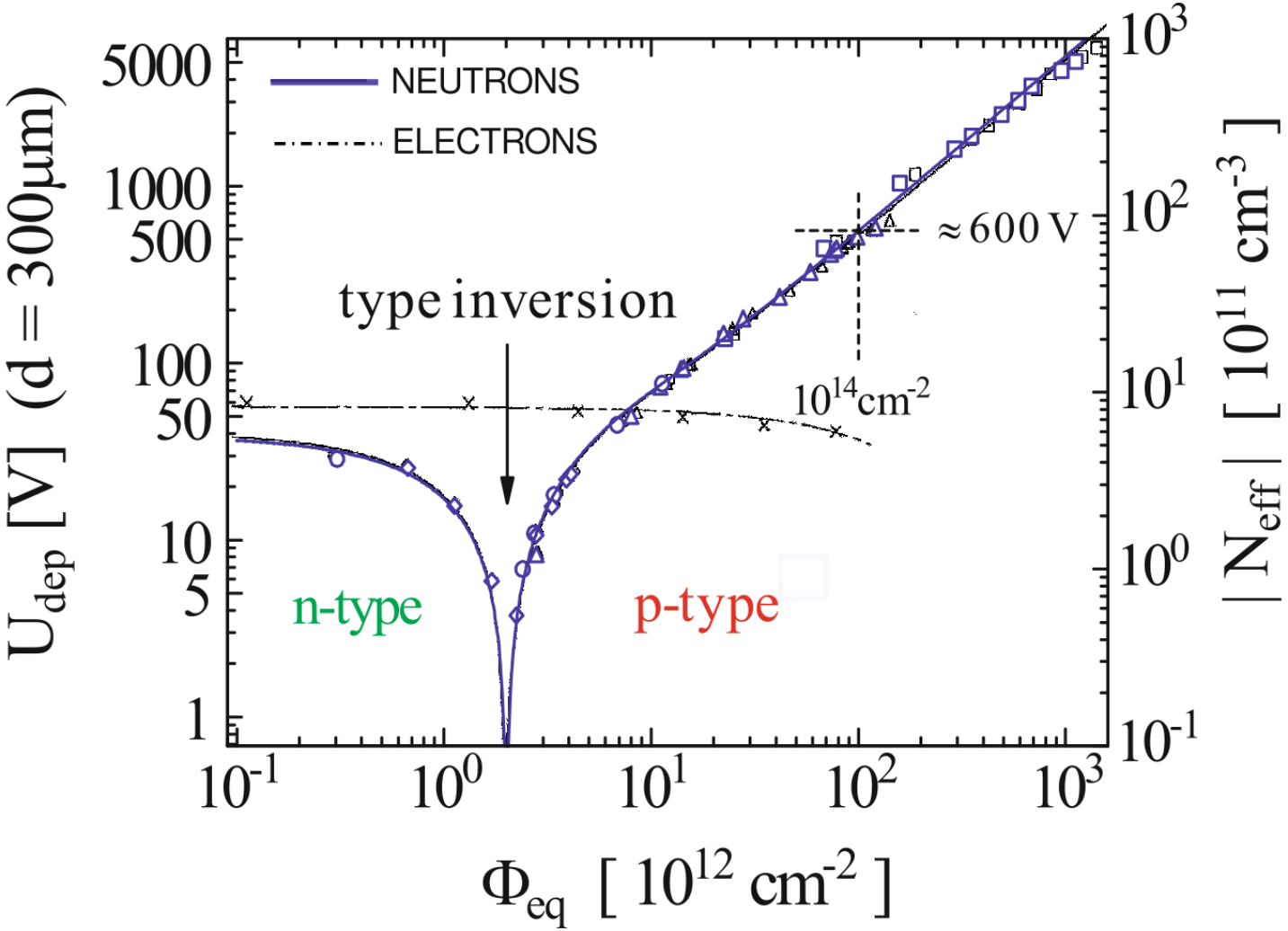

→ using of n-in-p instead of p-in-n microstrip sensors

Testing detectors

- Leakage current, current stability, humidity tests
- C_{bulk}
- C_{coup}
- C_{int}
- R_{int}
- R_{bias}
- PTP
- Visual inspection
- Metrology
- Full strip tests

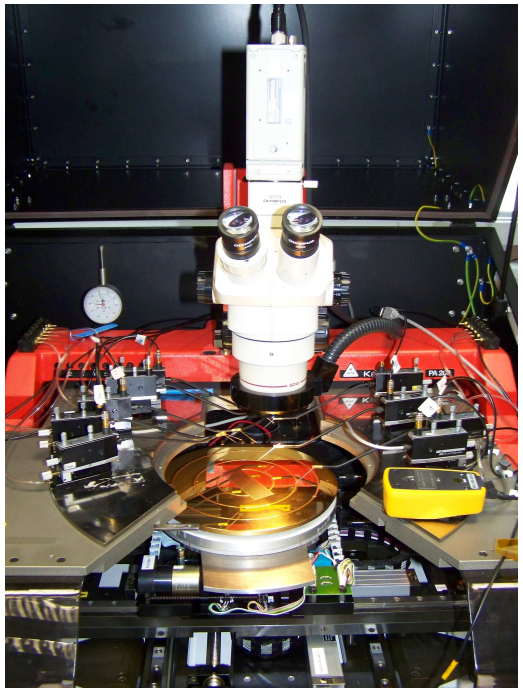

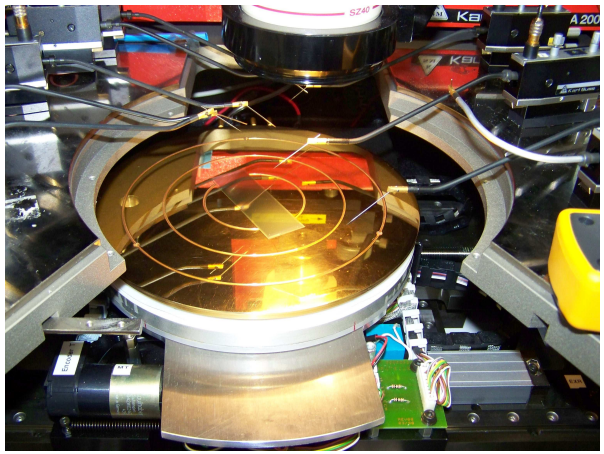

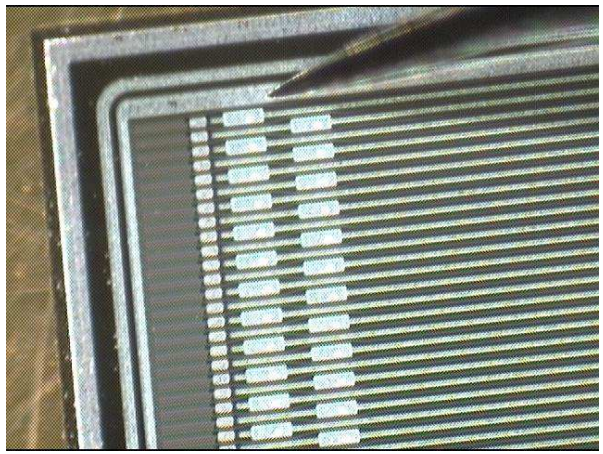

Testing detectors

- Leakage current, current stability, humidity tests
- C_{bulk}
- C_{coup}
- C_{int}
- R_{int}
- R_{bias}
- PTP
- Visual inspection
- Metrology
- Full strip tests

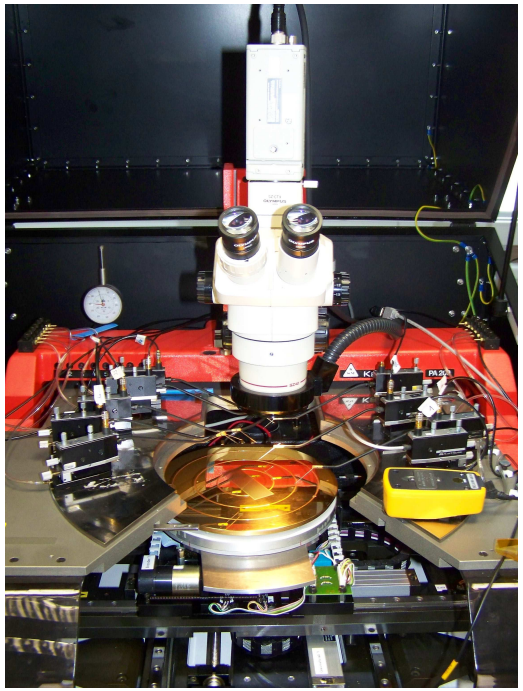

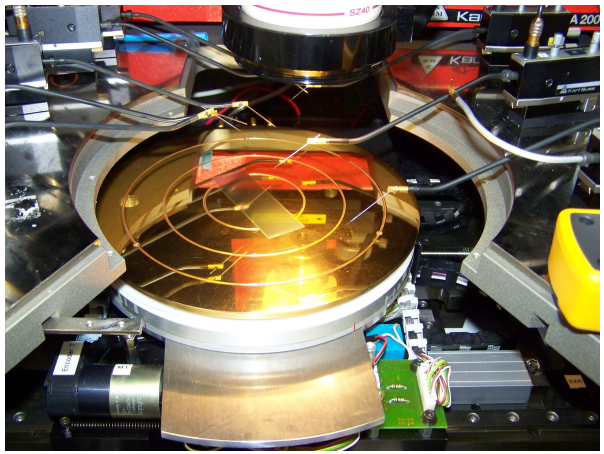

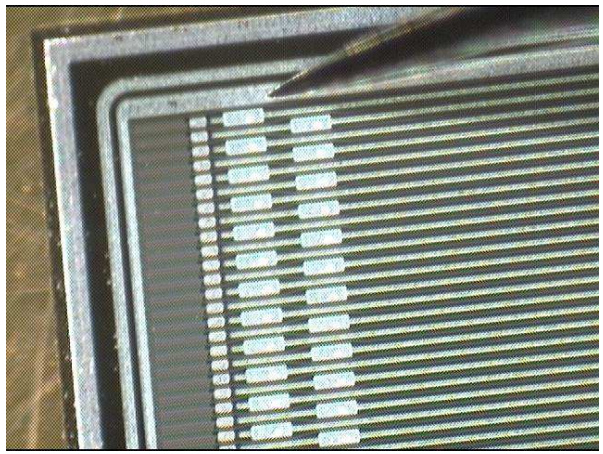

Leakage Current

- from generated electron-hole pairs in the silicon in the presence of an electric field
- source of noise in the final readout system

$\rightarrow$ should be kept as low as possible

- proportional to the depletion layer thickness
- for irradiated sensors depends linearly on the fluence
- temperature-dependent $\rightarrow$ cooling
- measured as IV - characteristics

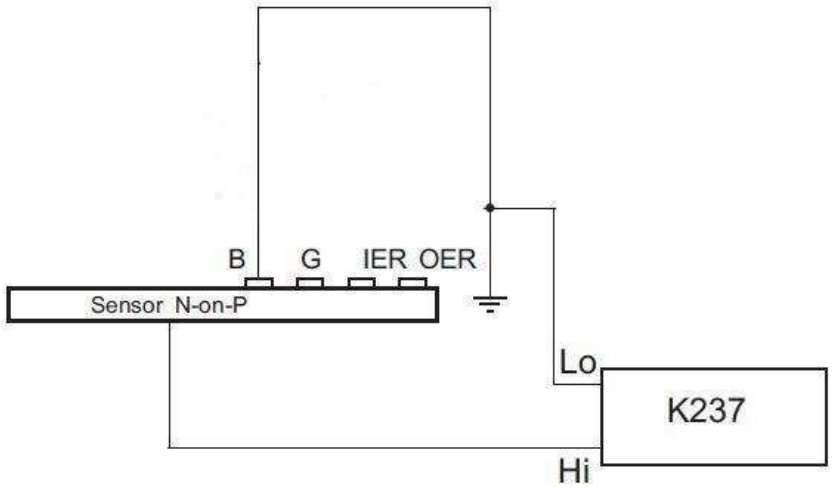

Bulk Capacitance

- capacitance formed between the backplane and the implant
- depletion layer acts like a parallel plate capacitor → can be used to determine FDV of the sensor
- FDV increases with irradiation

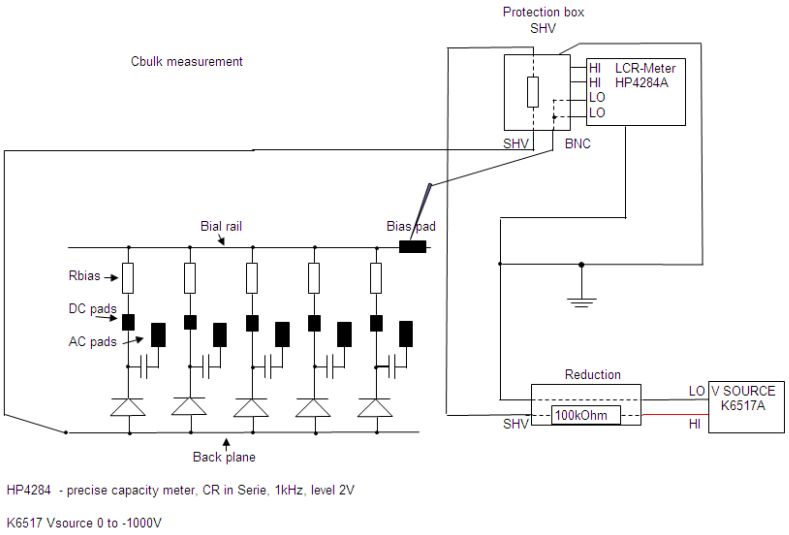

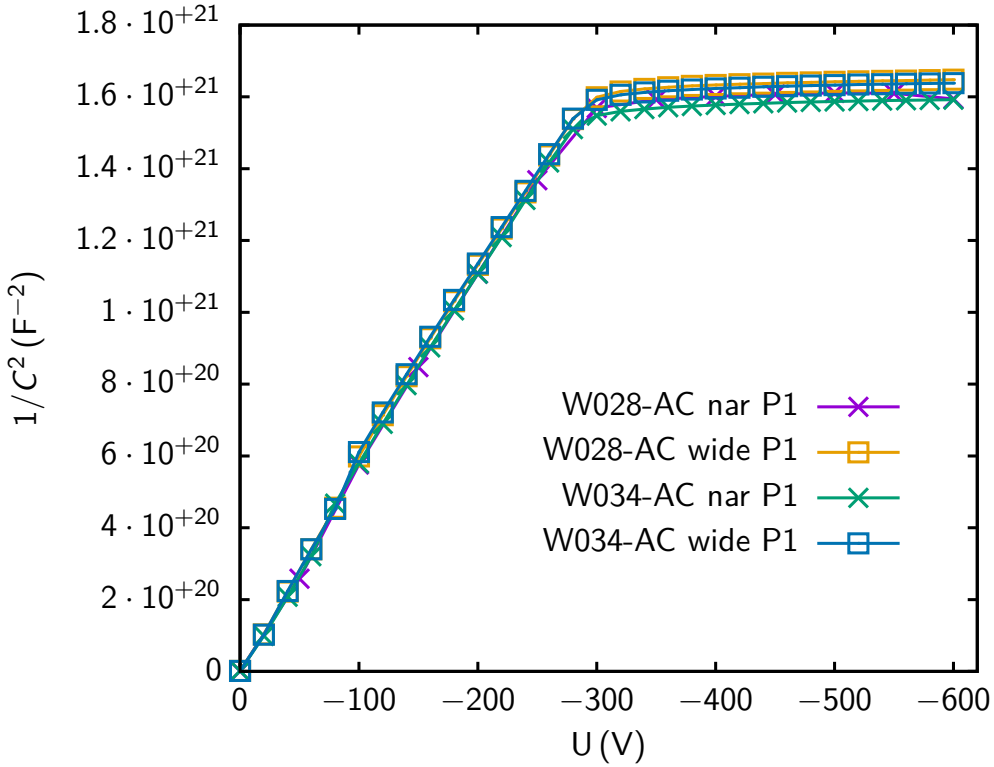

Coupling Capacitance

- between implant and top metal readout chip
- directly proportional to the charge created by the traversing particle

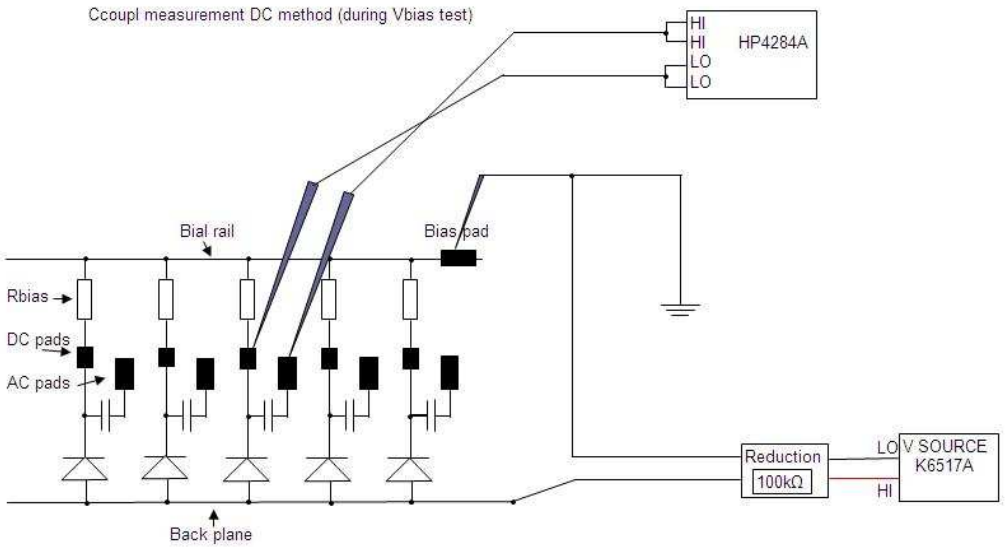

HP4284 - precise capacity meter, CR in parallel, 1kHz

K6517 Vsource 0 to -600V

Interstrip Capacitance

- capacitive coupling between strips can facilitate charge sharing
- dominates the input capacitance contributions to the front-end electronics
- determines noise level

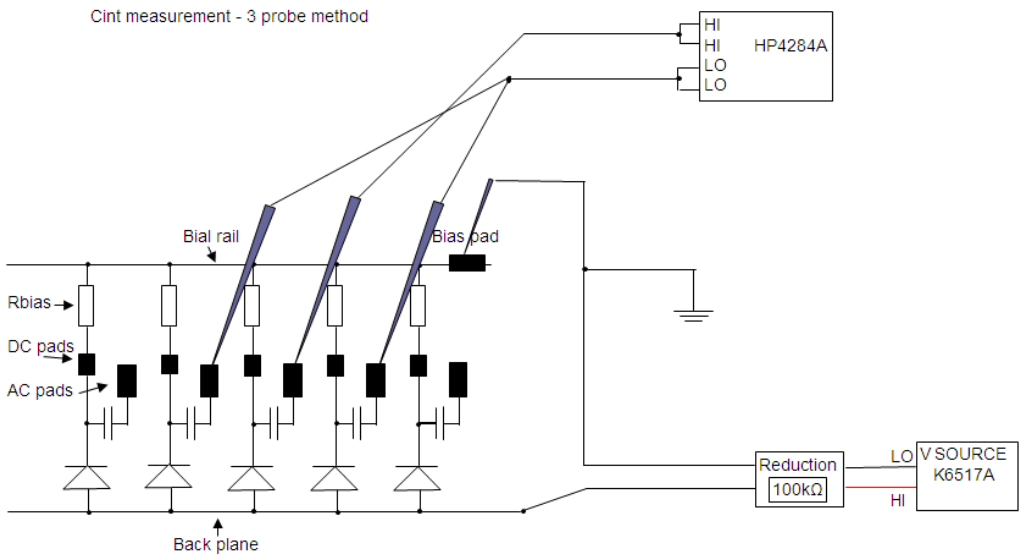

HP4284 - precise capacity meter, 1MHz, CPRP

K6517 Vsource 0 to -1000V

Interstrip Resistance

- resistance between neighboring strips
- high value ensures good strip isolation
- master voltage applied to outer DC strips, current measured on the middle strip

$$R_{\text{int}} = \frac{2}{\frac{\mathrm{d}I}{\mathrm{d}V_{\text{appl}}}}$$

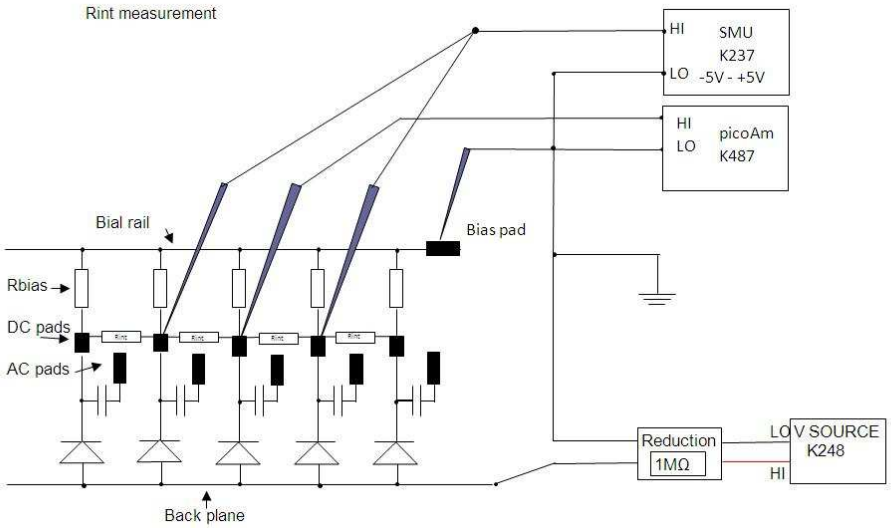

Bias Resistance

- polysilicon bias resistor connects the implant to the bias ring
- thermal noise contribution of the bias resistor $\rightarrow$ high value of R_{bias} needed
- 1-probe method (not irr.): test voltage applied between the implant (DC pad) and the grounded bias rail
- 3-probe method (irr.): test voltage applied on 2 DC pads, IV performed on the middle pad

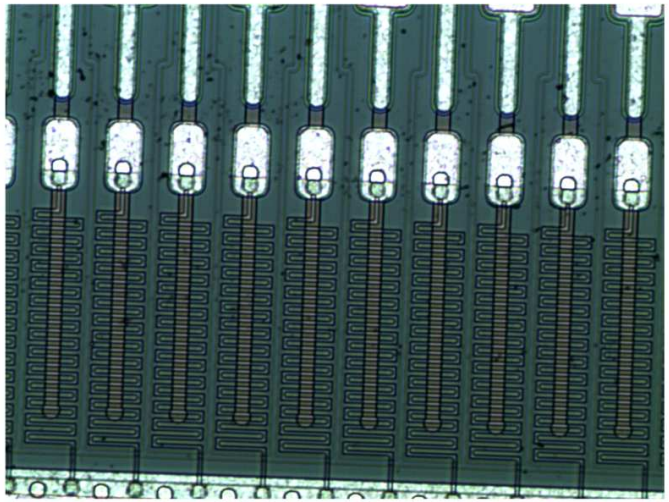

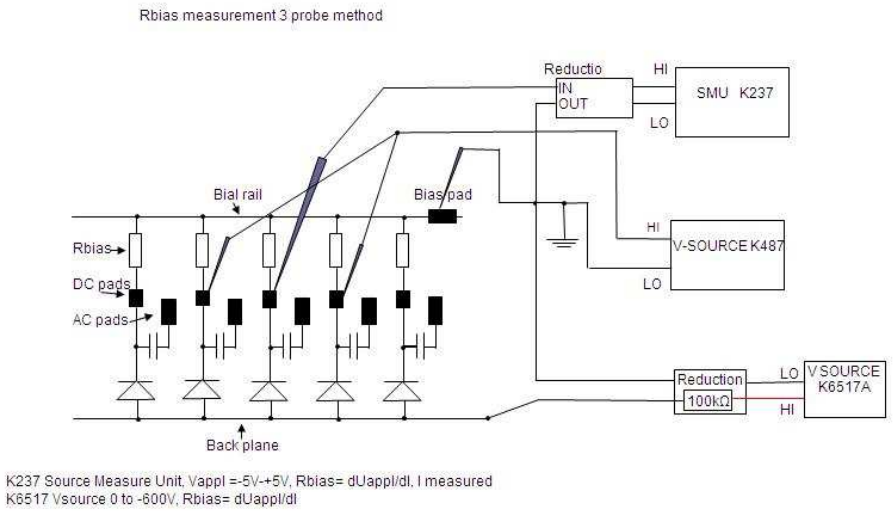

Punch-Through Protection Structure Performance

- protection against excessive charge liberated in the bulk
- alternative path for the excess charge to ground
- low resistance path parallel to the bias resistor activated when the voltage across the coupling capacitance (oxide) exceeds a certain value
- test voltage is applied between the implant and the grounded bias rail
- effective resistance is calculated from the resulting current and the test voltage

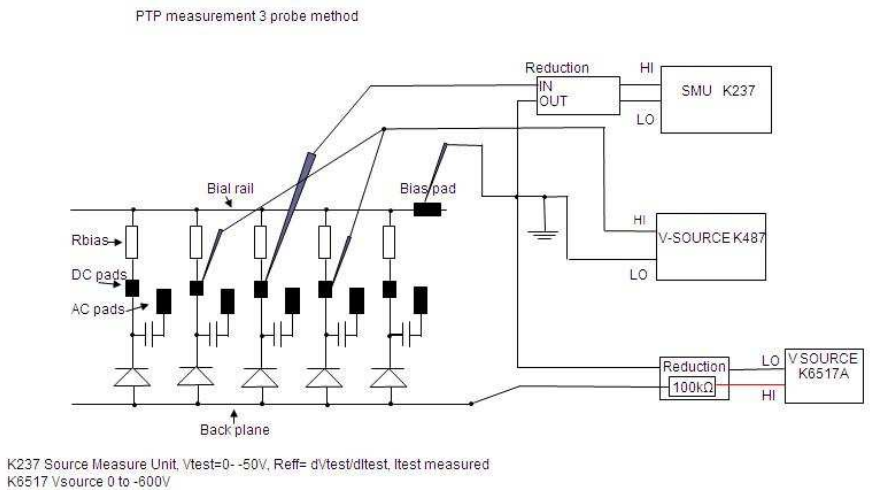

Tested Sensors

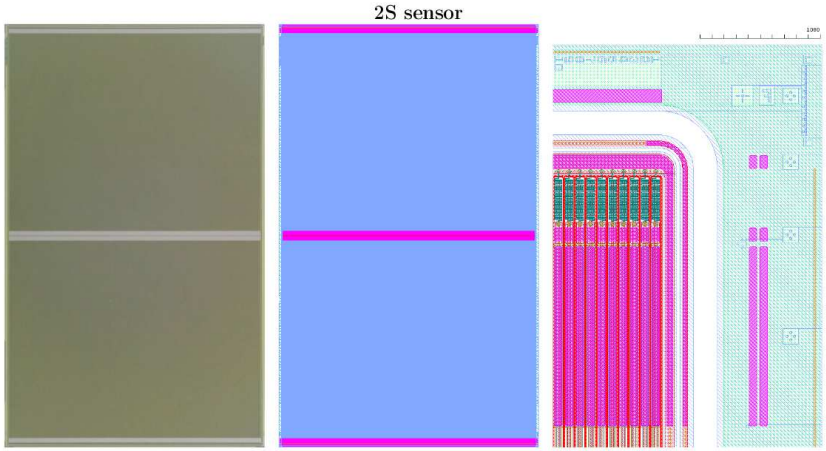

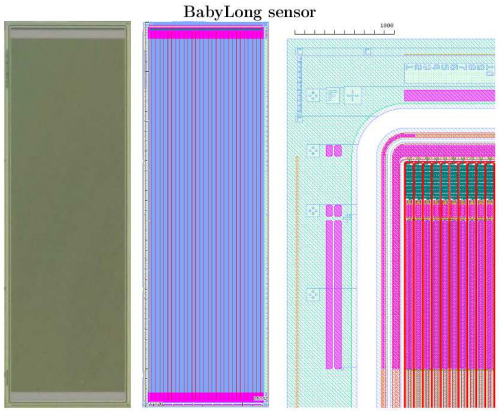

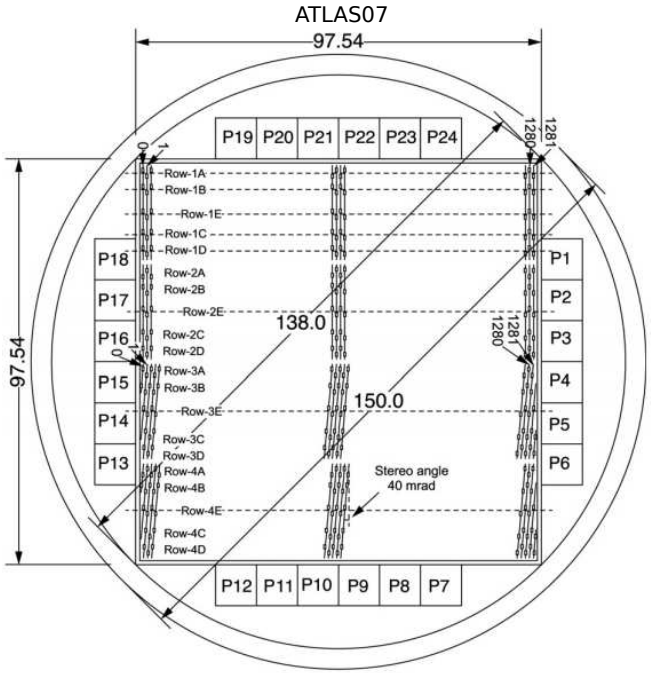

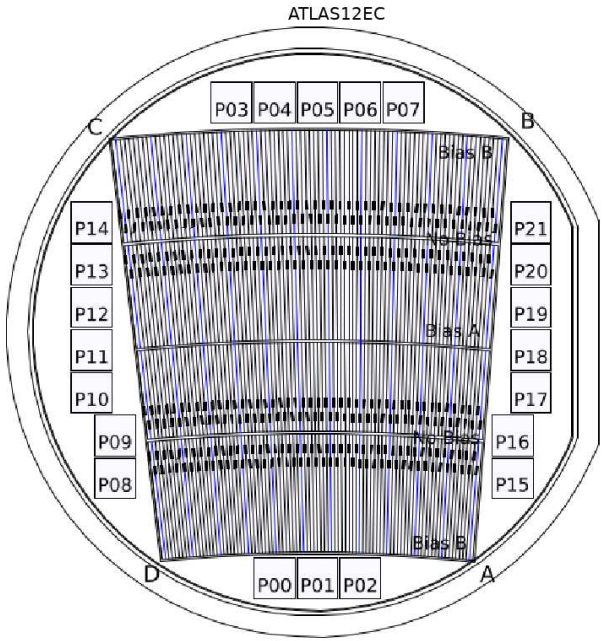

- Proton ($70\,\mathrm{MeV}$) irradiation (in $\mathrm{n_{eq}/cm^2}$) - CYRIC
- ATLAS12EC Mini Sensors
- Sample List

	$5.6 \cdot 10^{14}\,\mathrm{n_{eq}/cm^2}$	$1.1 \cdot 10^{15}\,\mathrm{n_{eq}/cm^2}$	$2.2 \cdot 10^{15}\,\mathrm{n_{eq}/cm^2}$
Default	W028 P1	W028 P2	W028 P3
Wide	W028 P2	W032 P2	W034 P2
Narrow	W028 P2	W031 P2	W034 P2

  and their not-irr. "friends"
- Measured Properties:
  - IV
    - not irr. $0 \approx 600\,\mathrm{V}$ at $T = 20\,^{\circ}\mathrm{C}$
    - irr. $0 \approx 1000\,\mathrm{V}$ at $T = -30\,^{\circ}\mathrm{C}$
  - CV (FDV)
  - R_{int}, R_{bias}, PTP
  - C_{coup}, C_{int}

Measurement Setup

Irr. sensors bonded to PCB board and tested in freezer. Not irr. sensors contacted by needles in the probe station.

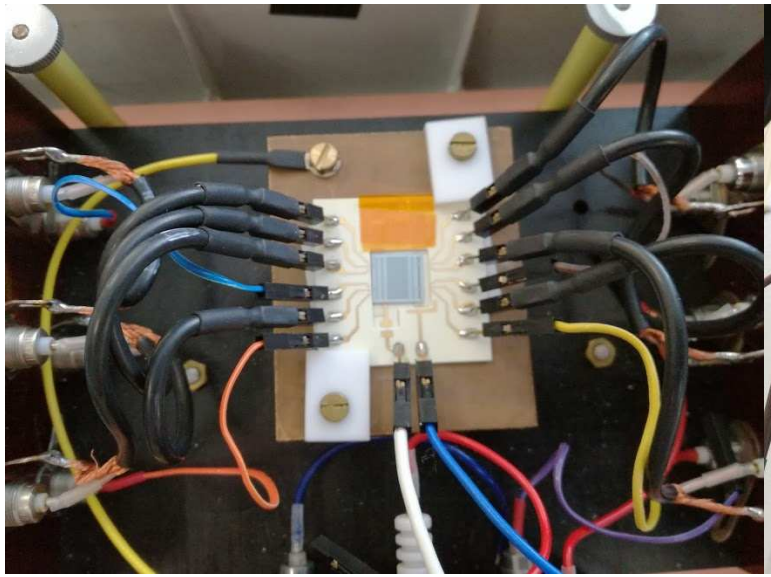

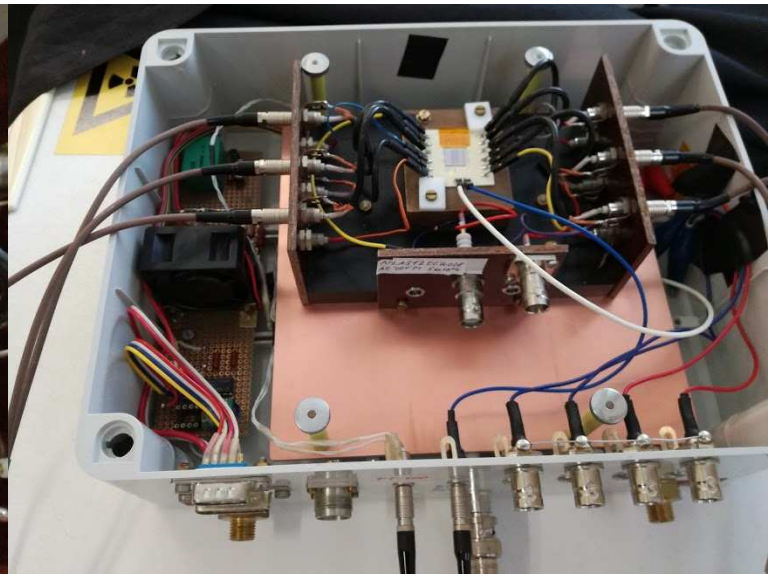

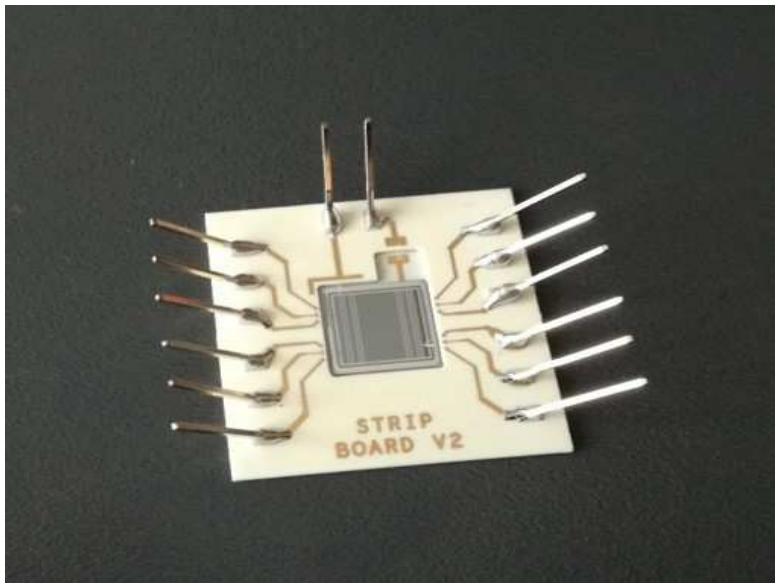

← Designed by Petr Mašek, IEAP, Czech Technical University, Prague

IV-Characteristics

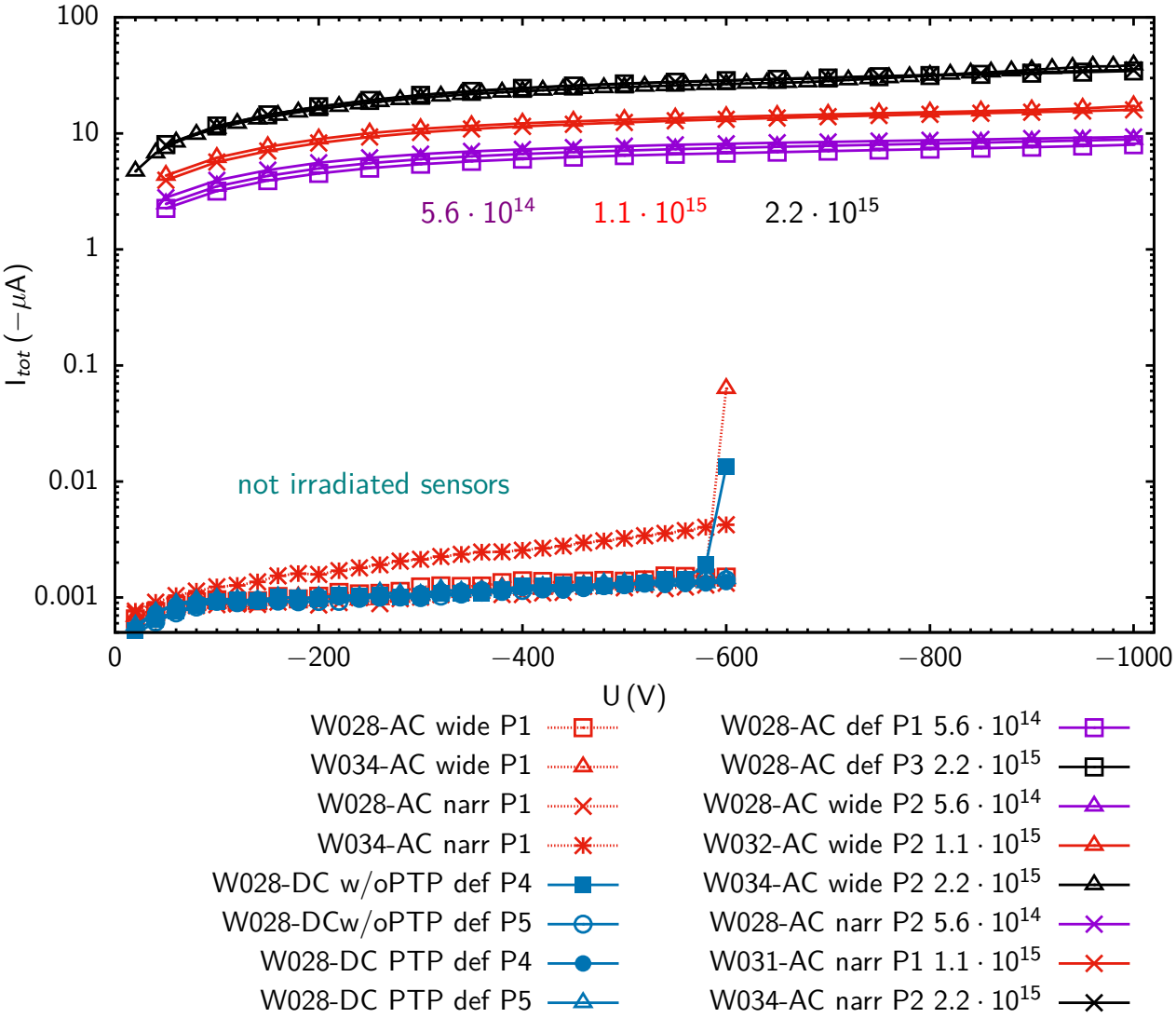

- not-irradiated sensors at $\approx 20\,^{\circ}\mathrm{C}$
- irradiated sensors at $\approx -30\,^{\circ}\mathrm{C}$

Results

- Not irr. sensors:
  - breakdown voltage occassionaly lower than 600 V for sensor measured immediately after being removed from dry atmosfere
- Irr. sensors:
  - smooth behaviour up to 1000 V
  - no break down voltage observed
  - current increase with proton irr. increase

- **Acceptance not irr. sensors:** below $0.1\,\mu\mathrm{A/cm^2}$ at 700 V at $20\,^{\circ}\mathrm{C}$ - our average value $\approx 0.003\,\mu\mathrm{A/cm^2}$ at 500 V ✓
- **Acceptance irr. sensors:** below 0.1 mA at 700 V (at $-20\,^{\circ}\mathrm{C}$) - our average values (0.01, 0.02, 0.05) $\mathrm{mA/cm^2}$ ✓

IV Characteristics for proton and gamma irradiated sensors

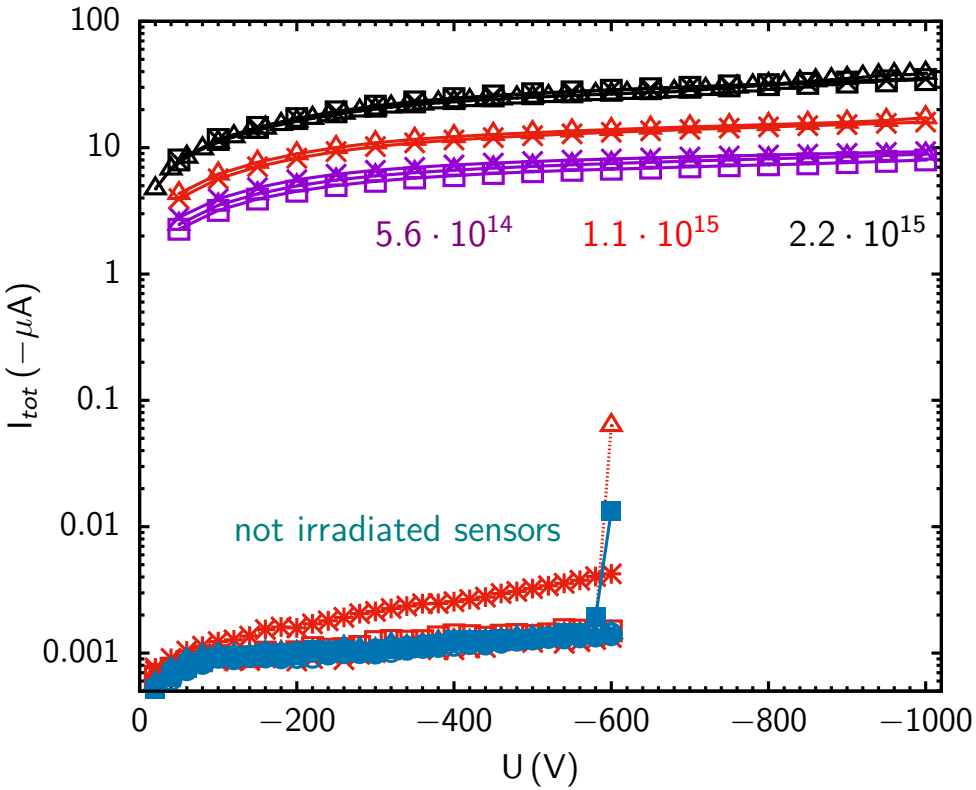

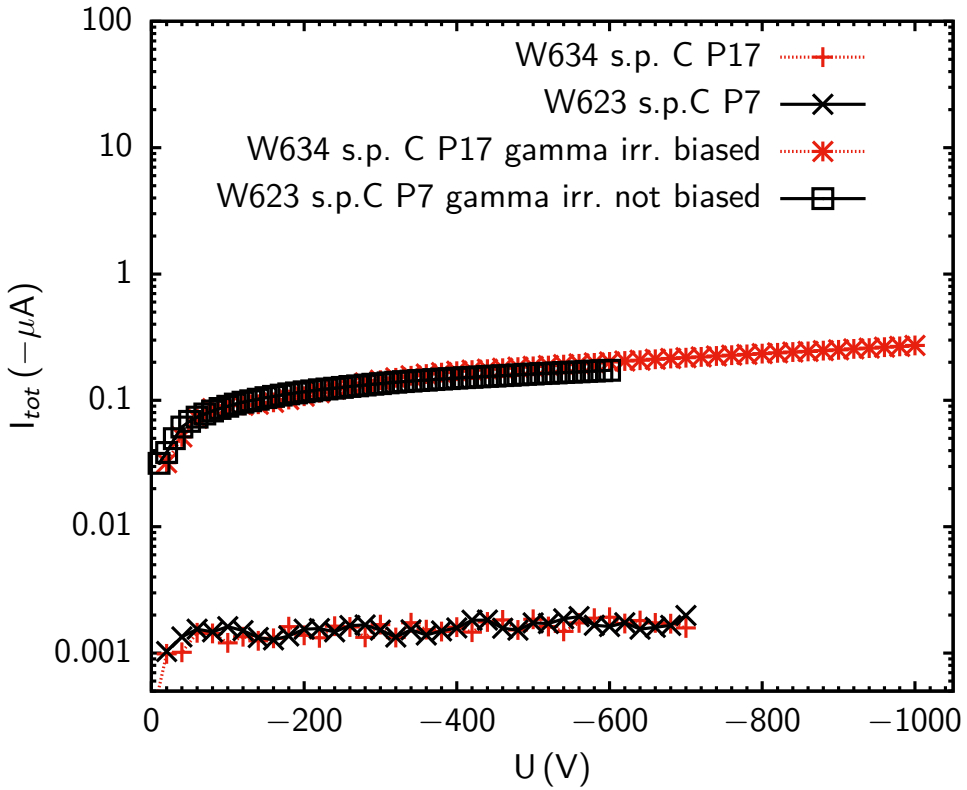

Humidity dependence

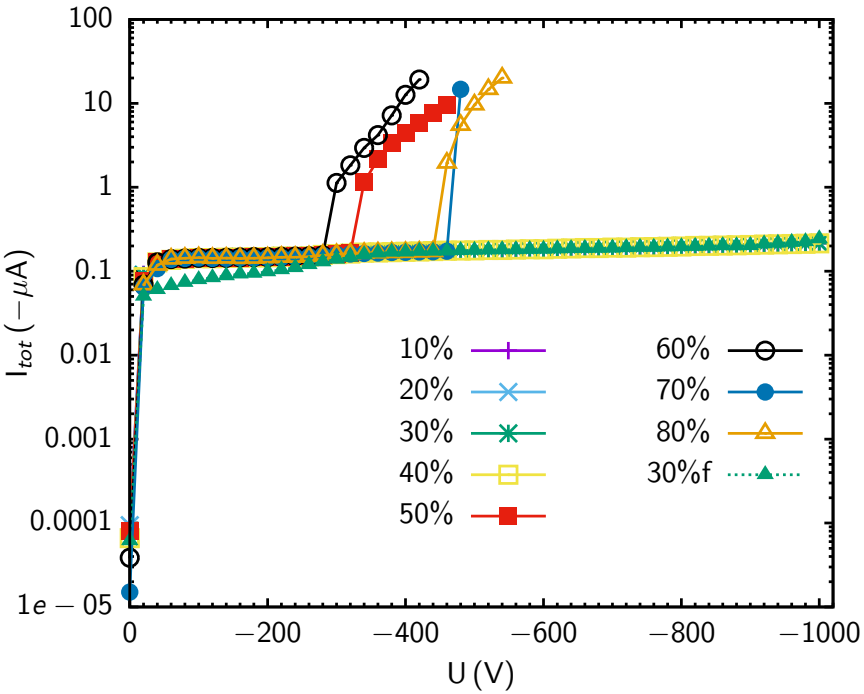

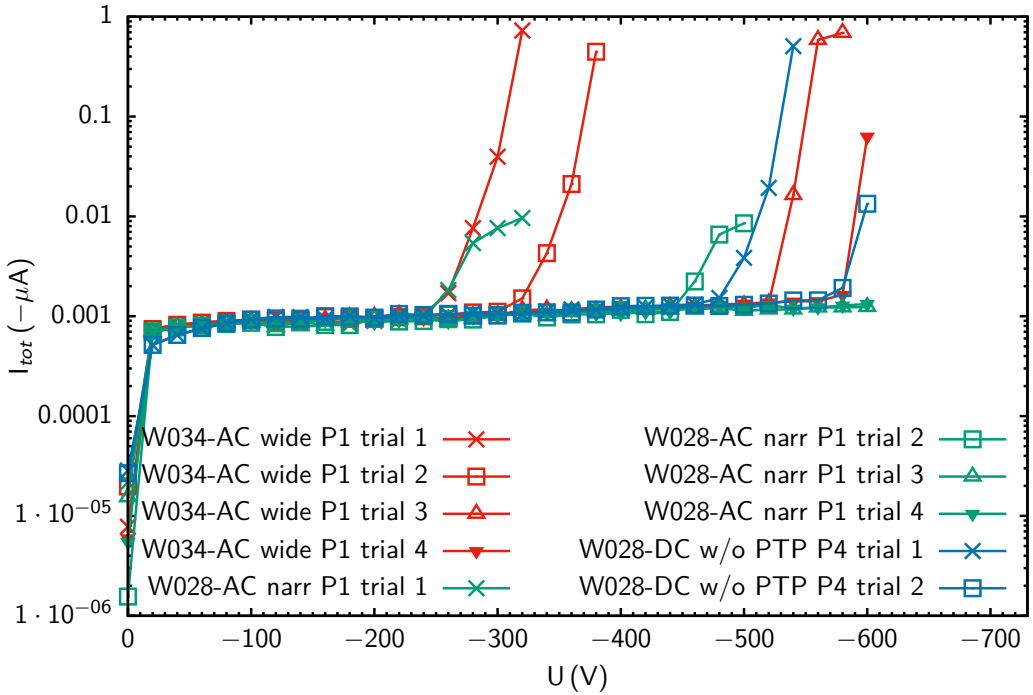

Results

- above 40 % RH early breakdown voltages appeared
- probably no permanent damage

Results

- sensors unstable if measured immediately after being removed from dry atmosphere to 30 % RH
- in the first trials early break-downs appeared
- with each new trial (or with the elapsed time), the break-down voltages were higher
- after $\approx$ 20 min most of the sensors improved to their usual IV characteristics

CV-Characteristics

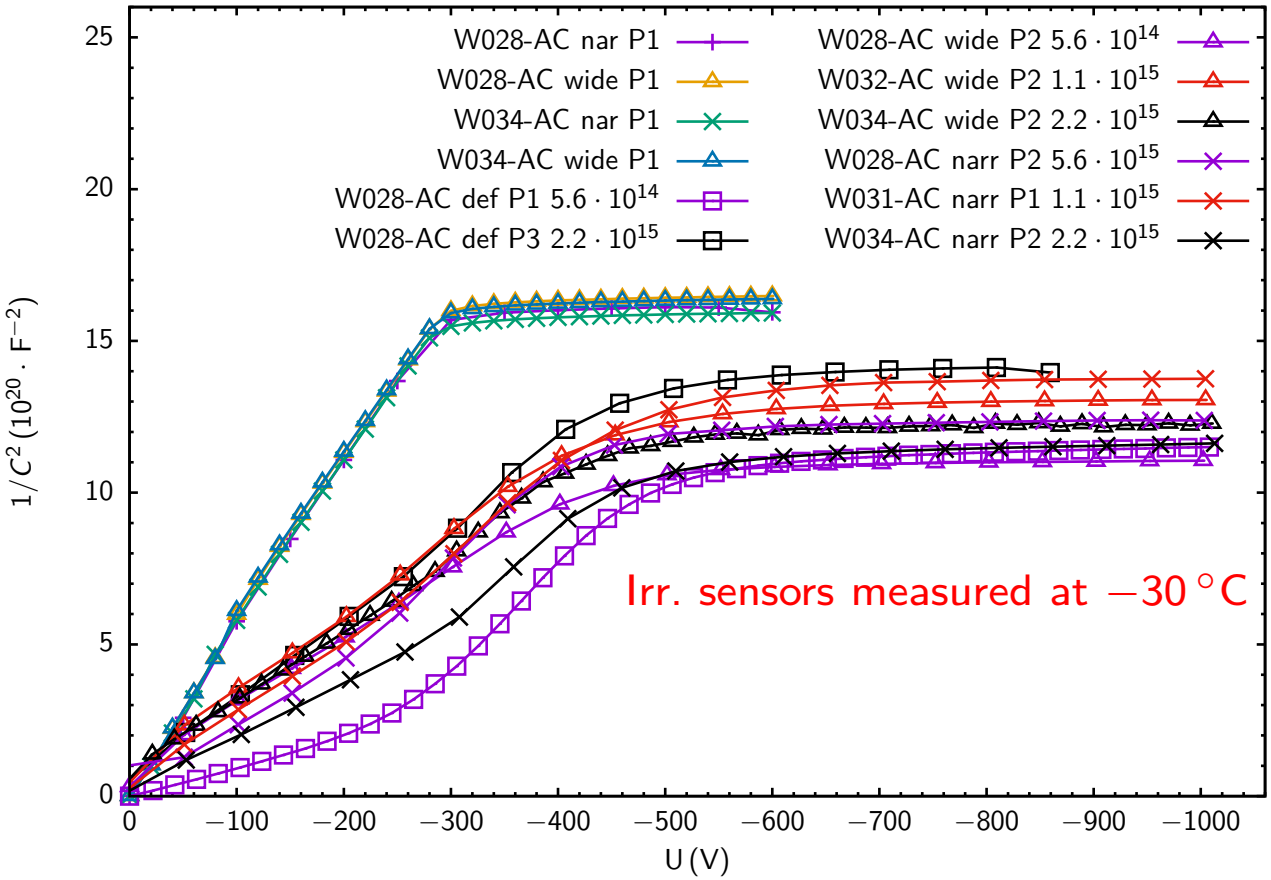

Results

- not irr. sensors
  FDV $\approx (281 - 288)$ V
- irr. $5.6 \cdot 10^{14}$
  FDV $\approx (446 - 460)$ V
- irr. $1.1 \cdot 10^{15}$
  FDV $\approx (452 - 490)$ V
- irr. $2.2 \cdot 10^{15}$
  FDV $\approx (453 - 585)$ V

CV-Characteristics and FDV

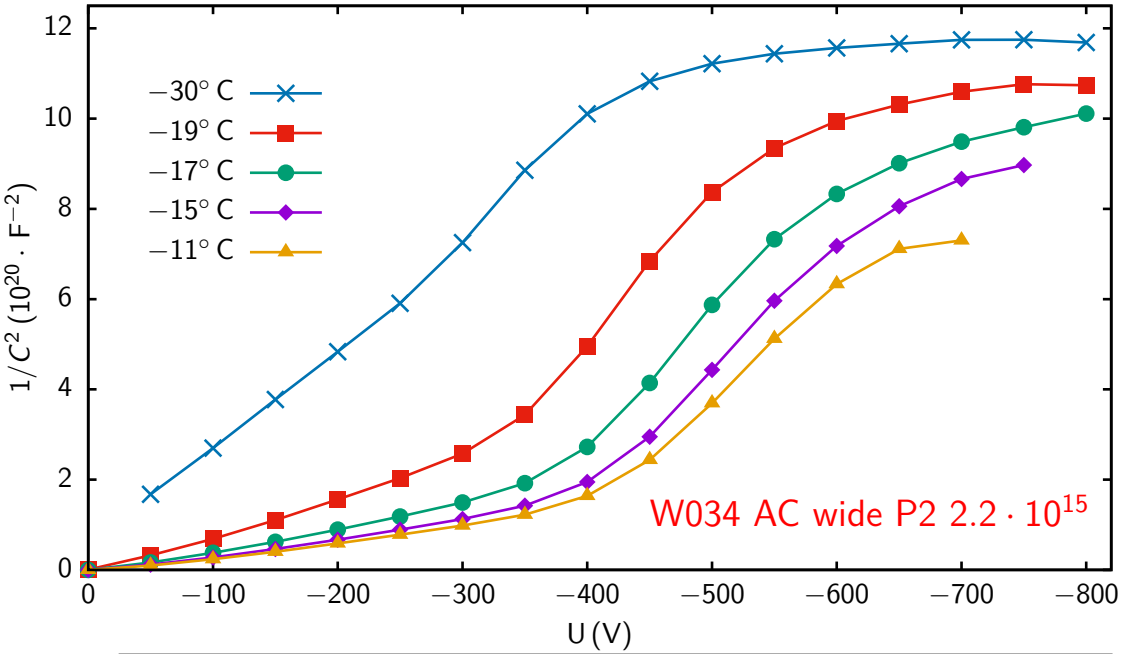

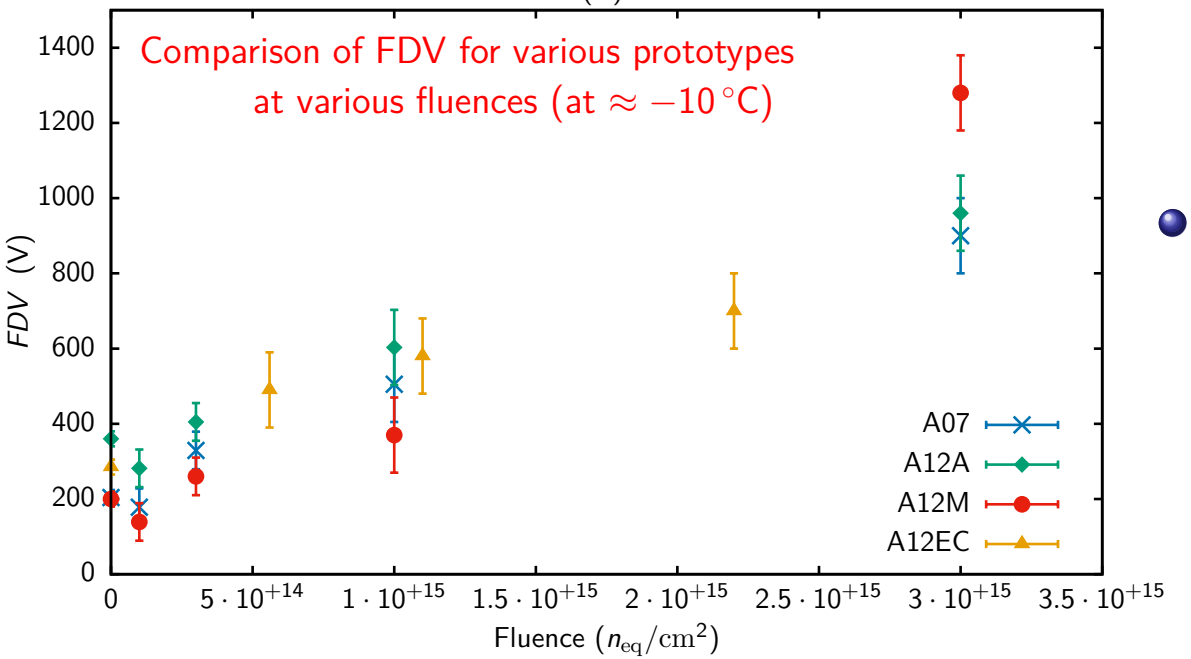

- CV curves of 1 sensor measured at different temperatures
  - ⇒ shape (bending) of curves changes with temperature
- dependence of full depletion voltage on fluence for A07, A12A, A12M, A12EC
  - ⇒ A12EC fit well among previous prototypes

Coupling Capacitance

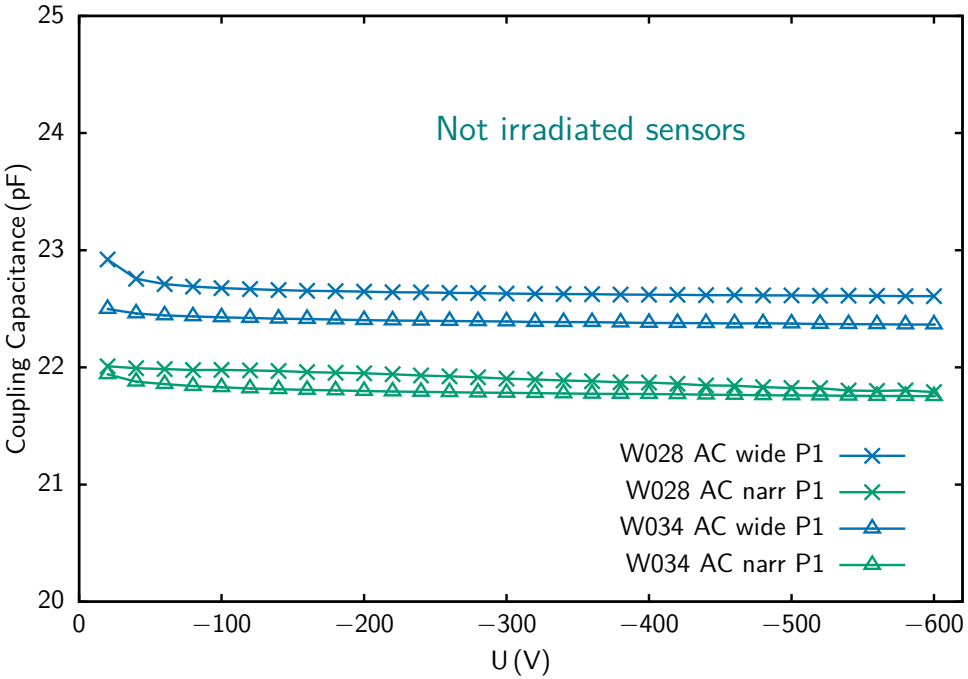

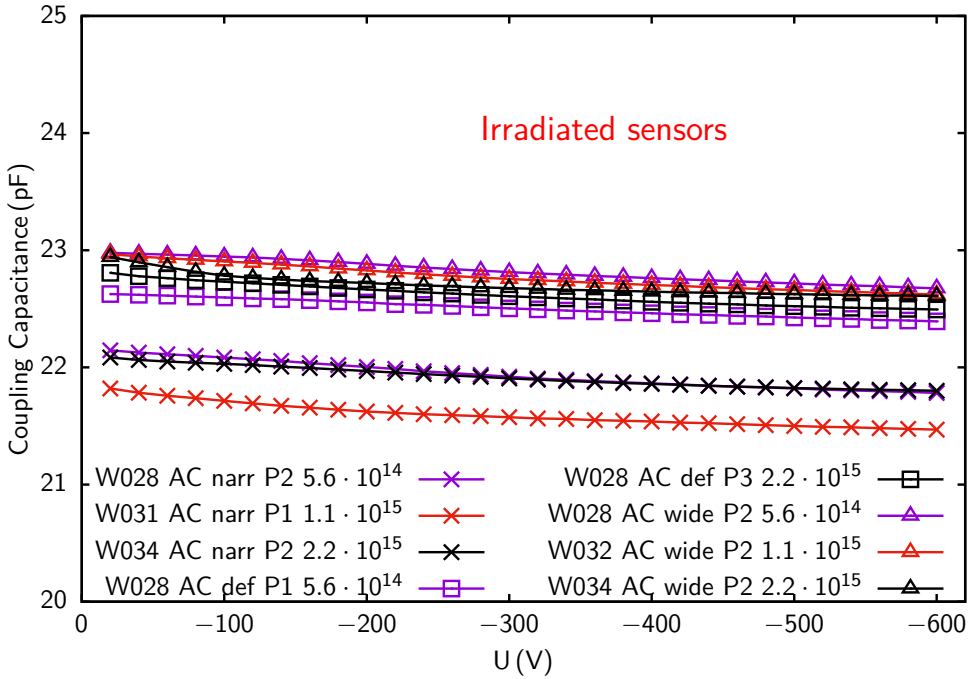

- Acceptance: $C_{\mathrm{coup}} \geq 20\,\mathrm{pF/cm}$
- not-irradiated sensors at $\approx 20\,^{\circ}\mathrm{C}$
- irradiated sensors at $\approx -30\,^{\circ}\mathrm{C}$

Results

- no radiation induced change of coupling capacitance observed
- not irr. sensors:
  - wide: $C_{\mathrm{coup}} = 22.5\,\mathrm{pF}$ (at 300 V) $\rightarrow 28.1\,\mathrm{pF/cm}$
  - narrow: $C_{\mathrm{coup}} = 21.8\,\mathrm{pF}$ (at 300 V) $\rightarrow 27.3\,\mathrm{pF/cm}$
- irr. sensors:
  - wide: $C_{\mathrm{coup}} = 22.8\,\mathrm{pF}$ (at 300 V) $\rightarrow 28.4\,\mathrm{pF/cm}$
  - default: $C_{\mathrm{coup}} = 22.7\,\mathrm{pF}$ (at 300 V) $\rightarrow 28.2\,\mathrm{pF/cm}$
  - narrow: $C_{\mathrm{coup}} = 21.8\,\mathrm{pF}$ (at 300 V) $\rightarrow 27.3\,\mathrm{pF/cm}$
- all sensors fulfill technical specifications

Interstrip Capacitance

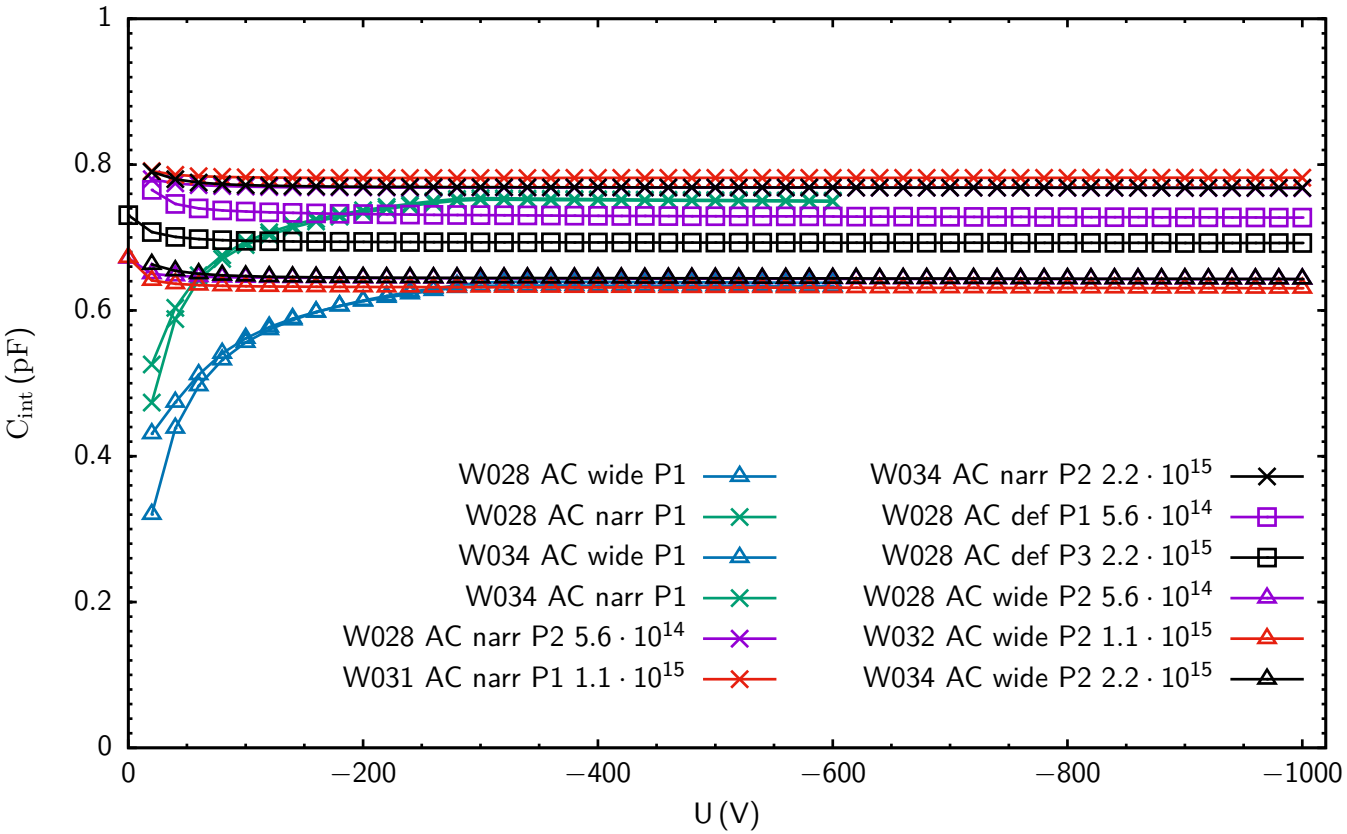

- Acceptance: $C_{\text{int}} \leq 1\,\text{pF/cm}$ at 300 V, measured at 100 kHz
- not-irradiated sensors at $\approx 20\,^{\circ}\text{C}$
- irradiated sensors at $\approx -30\,^{\circ}\text{C}$

Results

- no radiation induced change of interstrip capacitance observed
- not irr. sensors:
  - wide: $C_{\text{int}} = 0.64\,\text{pF}$ (at 300 V) $\rightarrow 0.79\,\text{pF/cm}$ ✓
  - narrow: $C_{\text{int}} = 0.75\,\text{pF}$ (at 300 V) $\rightarrow 0.94\,\text{pF/cm}$ ✓
- irr. sensors:
  - wide: $C_{\text{int}} = 0.64\,\text{pF}$ (at 300 V) $\rightarrow 0.80\,\text{pF/cm}$ ✓
  - default: $C_{\text{int}} = 0.71\,\text{pF}$ (at 300 V) $\rightarrow 0.89\,\text{pF/cm}$ ✓
  - narrow: $C_{\text{int}} = 0.76\,\text{pF}$ (at 300 V) $\rightarrow 0.95\,\text{pF/cm}$ ✓

Interstrip Resistance

- Not irr. acceptance: $R_{\mathrm{int}} > 10 \times R_{\mathrm{bias}}$ at $V_{\mathrm{bias}} = 300\,\mathrm{V}$
- Irr. acceptance: $R_{\mathrm{int}} > 10 \times R_{\mathrm{bias}}$ at $V_{\mathrm{bias}} = 400\,\mathrm{V}$

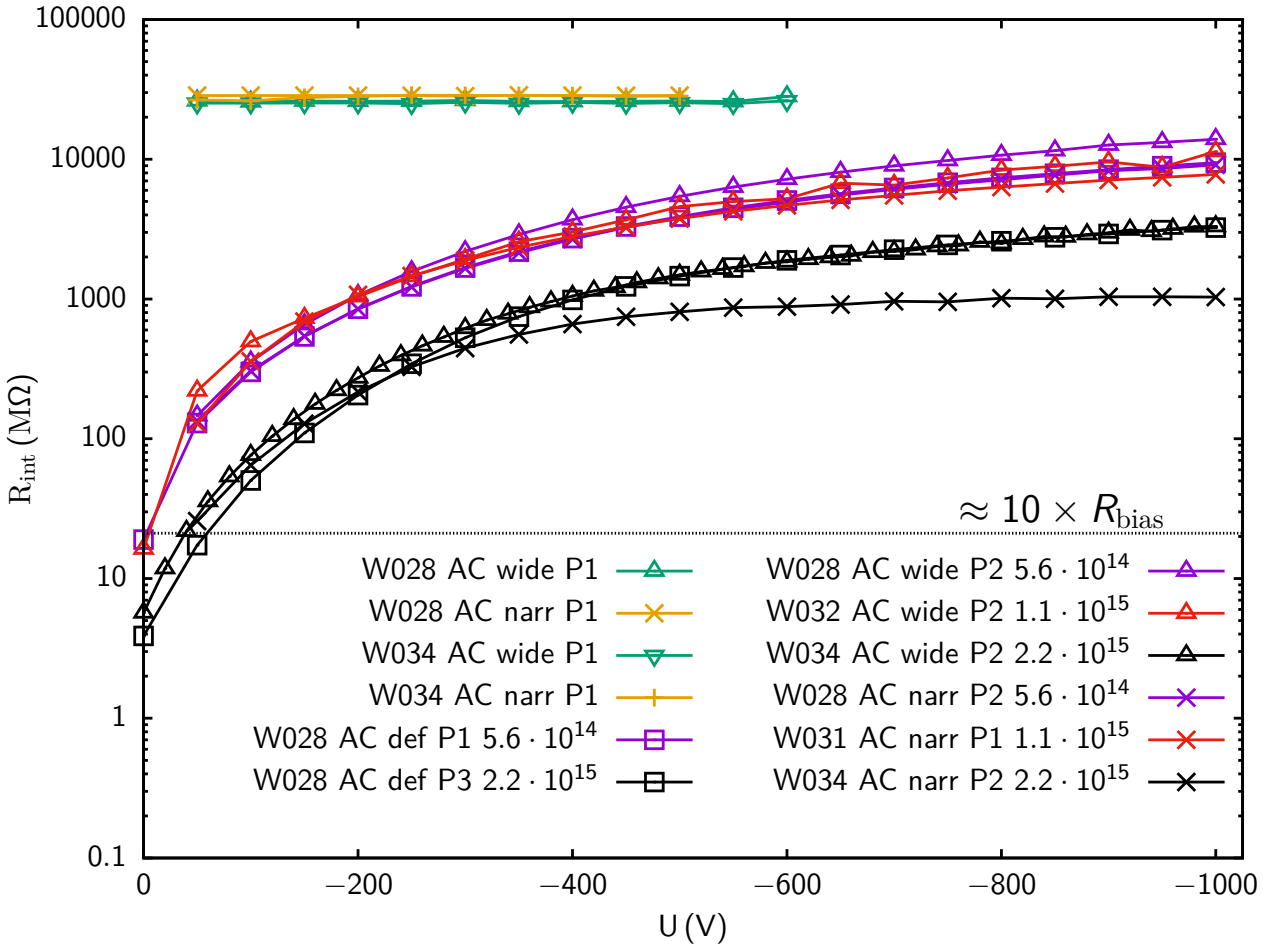

Results

- R_{int} fulfills techn. specs limit already at $V_{\mathrm{bias}} = 50\,\mathrm{V}$
- R_{int} for not irr. sensors is more than twice as high as R_{int} for irr. sensors

Interstrip Resistance - comparison of A07, A12A, A12M, A12EC

- $t = -20\,^{\circ}\mathrm{C}$, $V_{\mathrm{bias}} = -400\,\mathrm{V}$

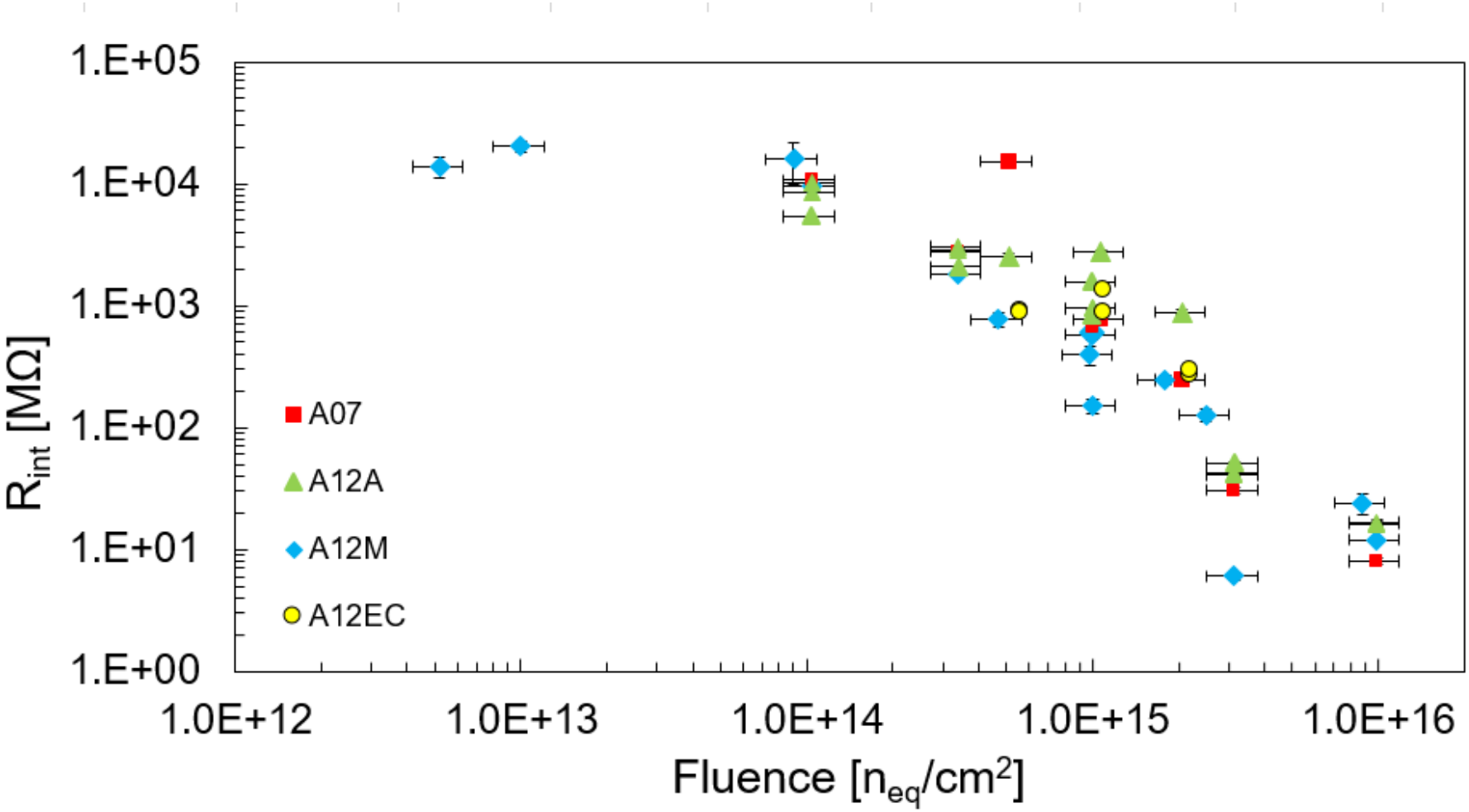

Results

- R_{int} of A12EC sensors fits perfectly among previous prototypes

Polysilicon Bias Resistance

- not irr.
  - $R_{\mathrm{bias}} \approx 1,5\,\mathrm{M\Omega}$ at $20\,^{\circ}\mathrm{C}$
  - $R_{\mathrm{bias}} \approx 1,8\,\mathrm{M\Omega}$ at $-30\,^{\circ}\mathrm{C}$
- irr. $R_{\mathrm{bias}} \approx (1,8 - 2,3)\,\mathrm{M\Omega}$ at $-30\,^{\circ}\mathrm{C}$

- temperature dependent
- grows slightly with increasing irr.

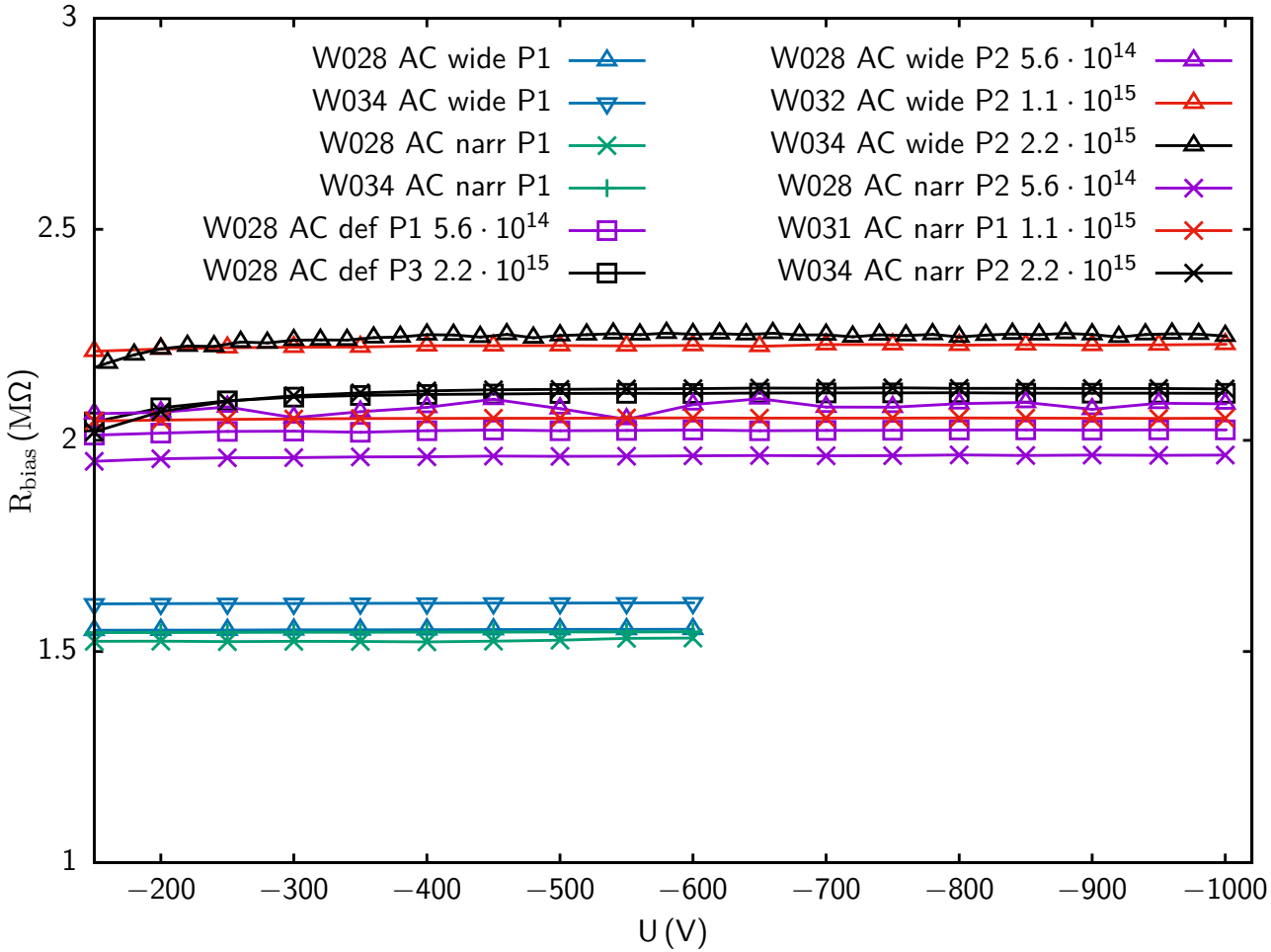

Punch-Through Protection Structure Performance

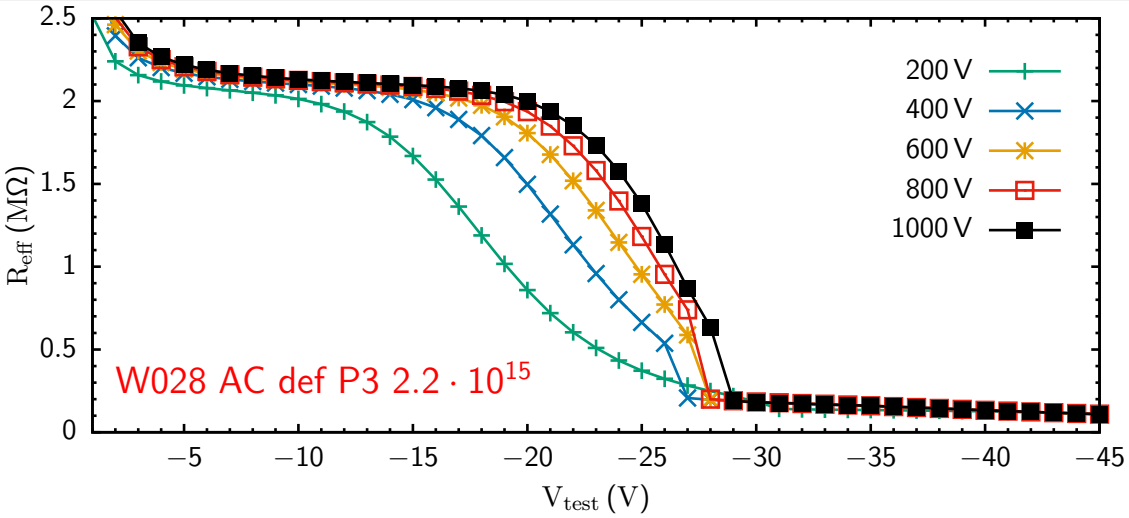

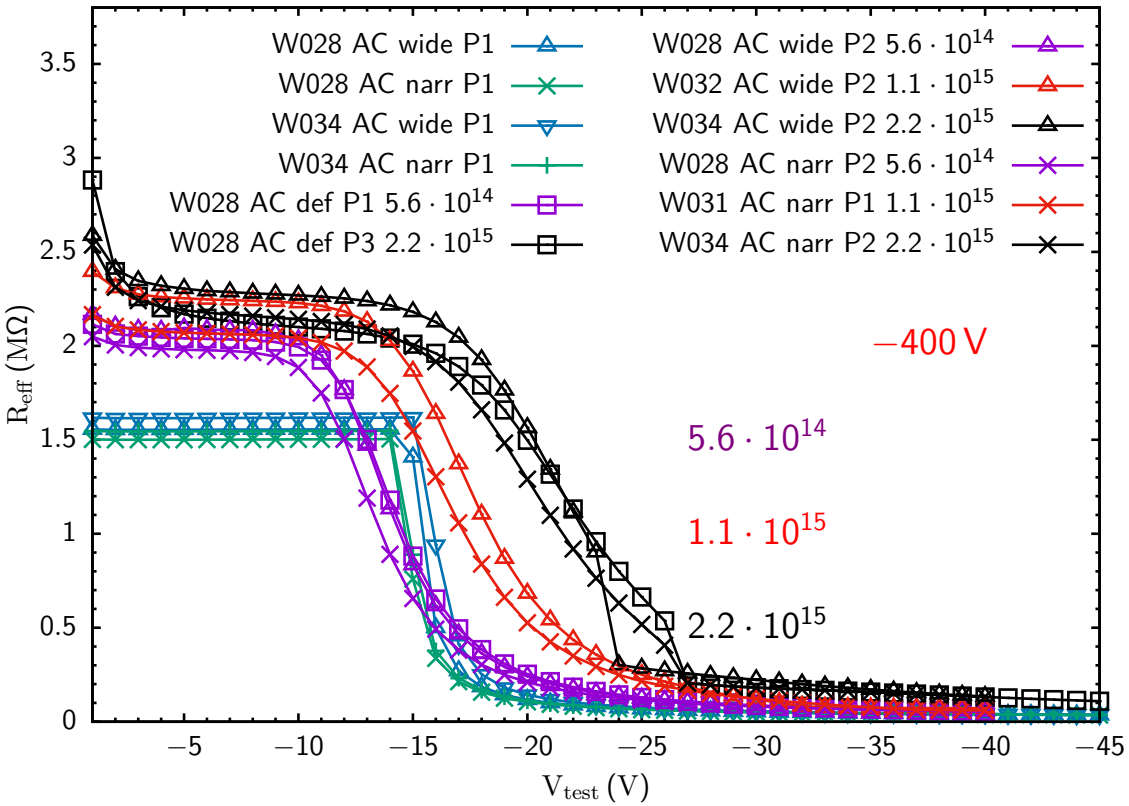

- measured resistance of PTP structure vs. voltage on implant for various bias voltages
- $R_{\mathrm{eff}} = \frac{V_{\mathrm{test}}}{I_{\mathrm{test}}}$
- both V_{PT} and V_{onset} for irr. sensors increase with increasing irr. and/or V_{bias}

V_{bias} (-V)	V_{onset} (-V) fluences ($\cdot 10^{15}\,\mathrm{n_{eq}/cm^2}$)			
	0	0.56	1.1	2.2
200	13.5	8.5	10	11
400	14.5	10	13	15
600	15.5	11	15	17.5
800		13.5	17	19
1000		15	17.5	20

V_{bias} (-V)	V_{PT} (-V) fluences ($\cdot 10^{15}\,\mathrm{n_{eq}/cm^2}$)			
	0	0.56	1.1	2.2
200	14	12	14.5	18.5
400	15.5	14	18	21
600	17	16	20	23.5
800		17.5	21.5	24
1000		19.5	23	24.5

Summary

- LHC $\rightarrow$ HL-LHC
- replacement of the ATLAS ID by a new all-silicon ITk

$\rightarrow$ high resolution

$\rightarrow$ radiation hardness

- sensor studies
  - measured properties of new ATLAS12EC sensors fulfill technical specifications and are in good agreement with results from University of Tsukuba
  - obtained values for FDV & R_{int} are consistent with A07, A12A, A12M sensors

Thank You for Your Attention

Questions?

Summary

- LHC $\rightarrow$ HL-LHC
- replacement of the ATLAS ID by a new all-silicon ITk

$\rightarrow$ high resolution

$\rightarrow$ radiation hardness

- sensor studies
  - measured properties of new ATLAS12EC sensors fulfill technical specifications and are in good agreement with results from University of Tsukuba
  - obtained values for FDV & R_{int} are consistent with A07, A12A, A12M sensors

Thank You for Your Attention

Questions?

Summary

- LHC $\rightarrow$ HL-LHC
- replacement of the ATLAS ID by a new all-silicon ITk

$\rightarrow$ high resolution

$\rightarrow$ radiation hardness

- sensor studies
  - measured properties of new ATLAS12EC sensors fulfill technical specifications and are in good agreement with results from University of Tsukuba
  - obtained values for FDV & R_{int} are consistent with A07, A12A, A12M sensors

Thank You for Your Attention

Questions?

Summary

- LHC $\rightarrow$ HL-LHC
- replacement of the ATLAS ID by a new all-silicon ITk

$\rightarrow$ high resolution

$\rightarrow$ radiation hardness

- sensor studies
  - measured properties of new ATLAS12EC sensors fulfill technical specifications and are in good agreement with results from University of Tsukuba
  - obtained values for FDV & R_{int} are consistent with A07, A12A, A12M sensors

Thank You for Your Attention

Questions?

Schemes

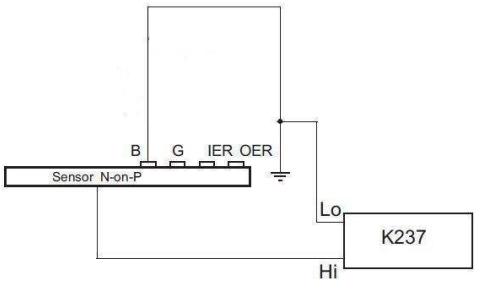

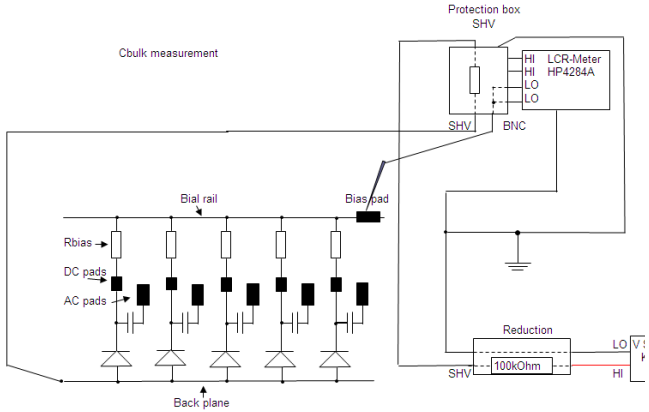

HP4284 - precise capacity meter, CR in Serie, 1kHz, level 2V

K6517 Vsource 0 to -1000V

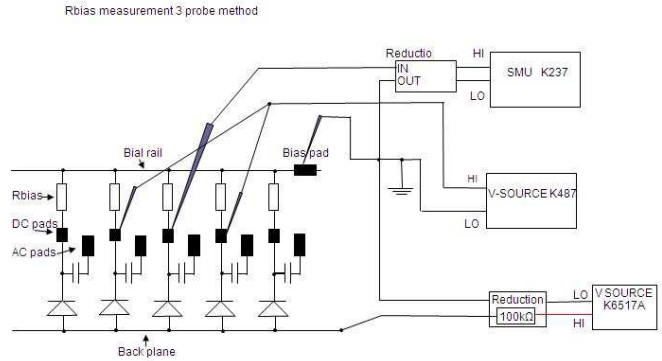

K237 Source Measure Unit, Vappl =-5V-+5V, Rbias= dUappl/dI, I measured

K6517 Vsource 0 to -600V, Rbias= dUappl/dI

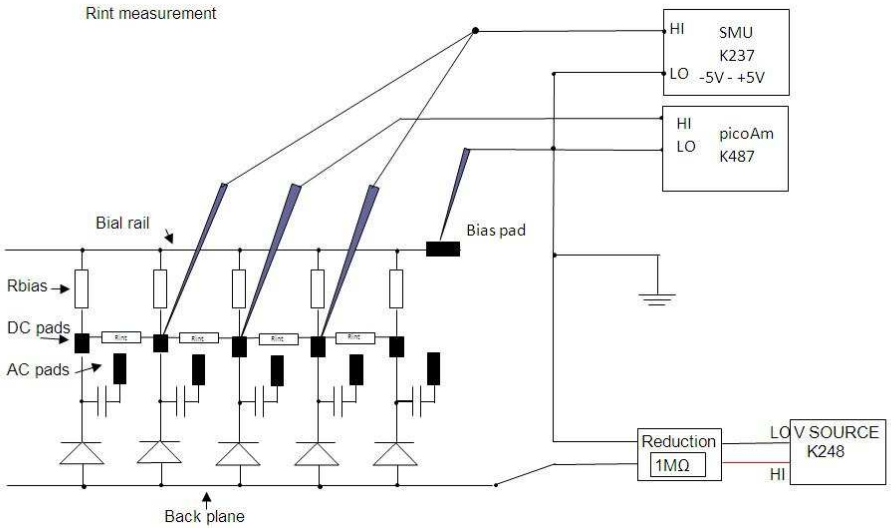

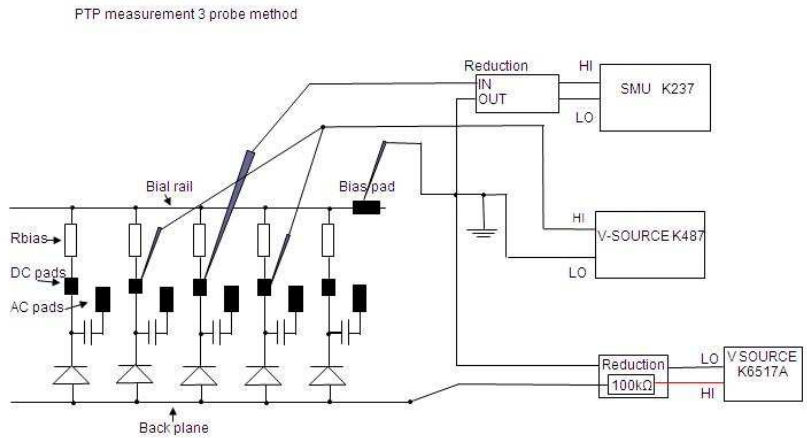

K237 Source Measure Unit, Vtest=0- -50V, Reff= dVtest/dItest, Itest measured

K6517 Vsource 0 to -600V

IV-Characteristics 2

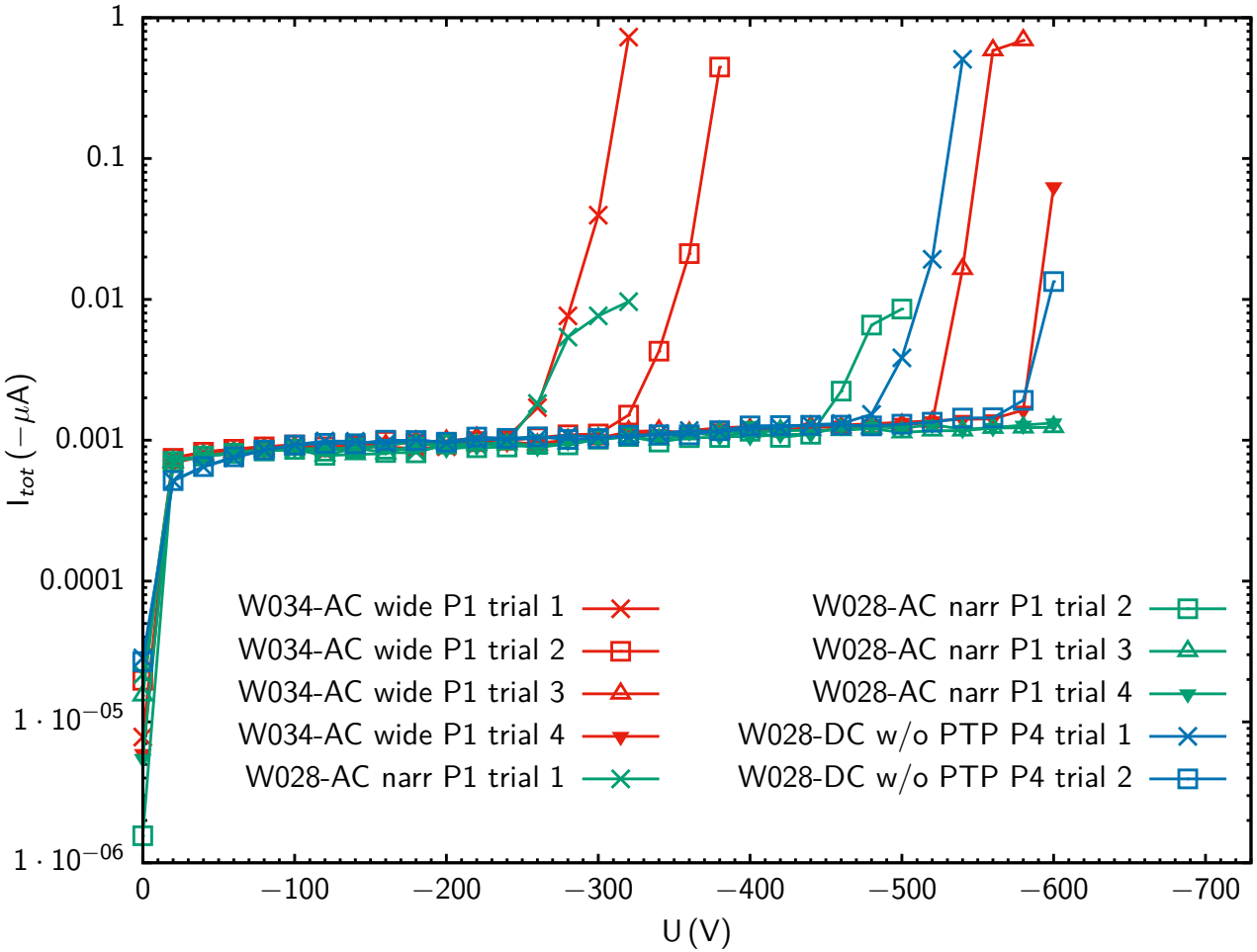

- not irr. sensors were kept in dry storage cabinet at low humidity (RH $\approx$ 1.5 %)
- measurements were taken at RH $\approx$ 30 %

Results

- sensors unstable if measured immediately after being removed from dry atmosphere to 30 % RH
- in the first trials early break-downs appeared
- with each new trial (or with the elapsed time), the break-down voltages were higher
- after $\approx$ 20 min most of the sensors improved to their usual IV characteristics

Leakage current vs proton Fluence comparison: A07, A12A, A12M and A12EC

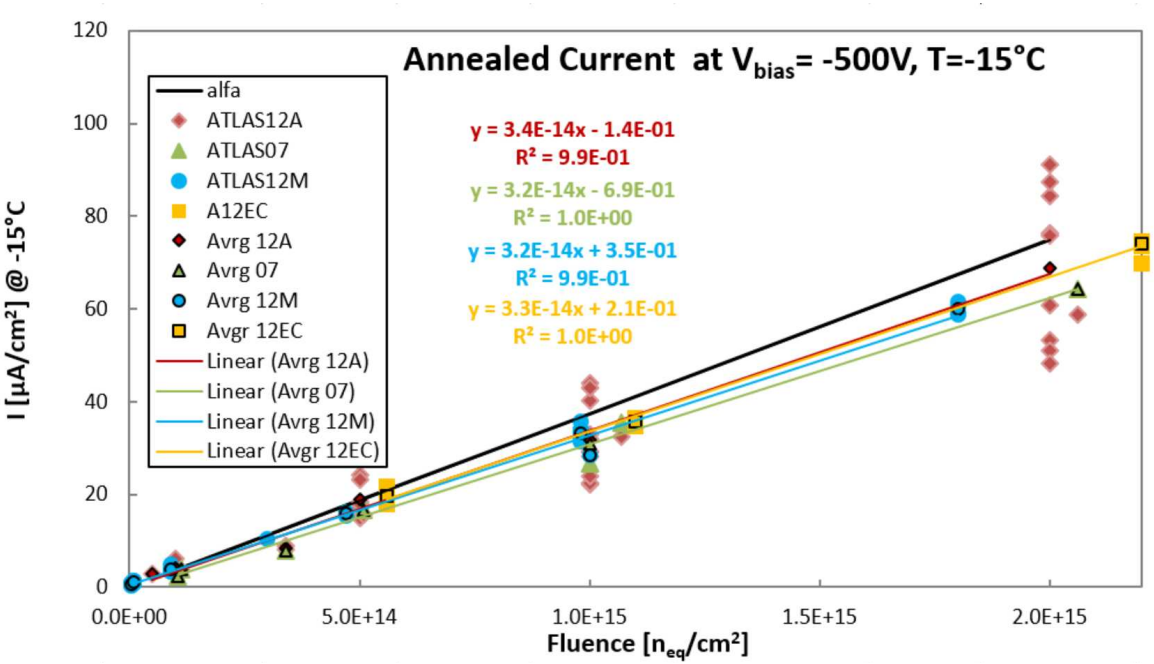

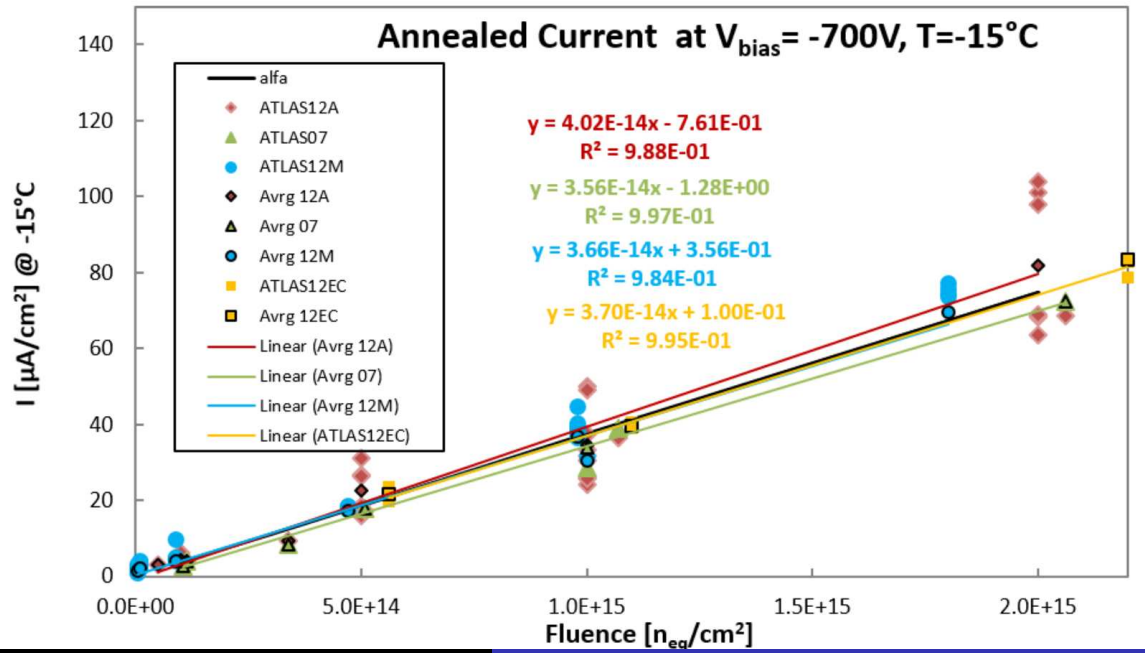

- current normalized to $1\,\mathrm{cm}^2$ area;
- active area - inner dimension of bias ring A(ATLAS12EC) $= 0.637\,\mathrm{cm}^2$
- temperature normalized to $-15\,^{\circ}\mathrm{C}$ $I(T_{-15}) = I(T_{\mathrm{M}}) \cdot (T_{-15}/T_{\mathrm{M}})^2$ $\exp(-E/2k_B \cdot (1/T_{-15} - 1/T_{\mathrm{M}}))$, with $E = 1.2\,\mathrm{eV}$
- $\alpha(+20\,^{\circ}\mathrm{C}) = 4 \cdot 10^{-17}\,\mathrm{A/cm}$, temperature correction coefficient between $+20\,^{\circ}\mathrm{C}$ and $-15\,^{\circ}\mathrm{C}$: 33

Result

- currents of A12EC consistent with A07, A12A, A12M

First tests

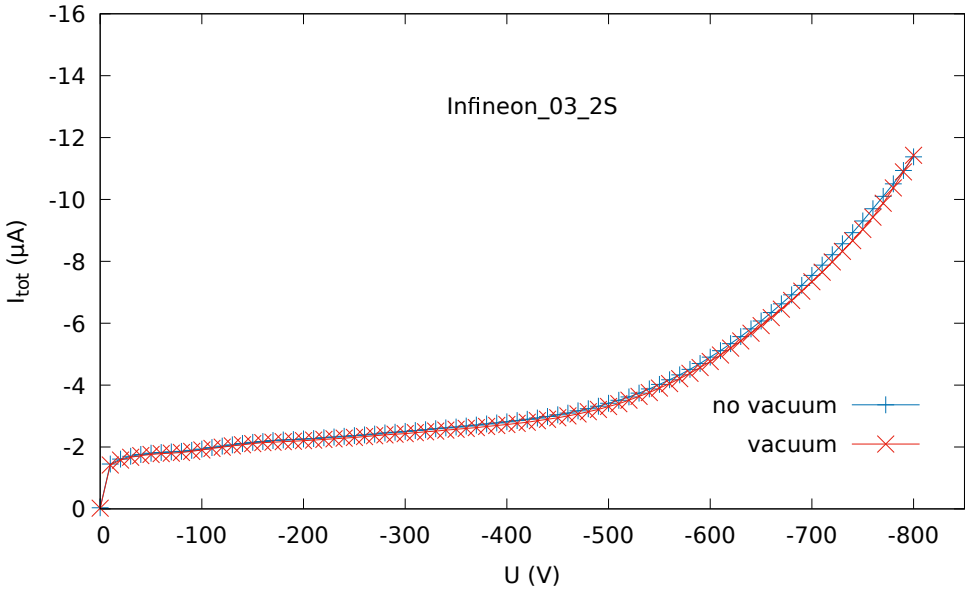
Infineon_03_2S
no vacuum
vacuum
I_{tot} (µA)
U (V)
-16
-14
-12
-10
-8
-6
-4
-2
0
0
-100
-200
-300
-400
-500
-600
-700
-800

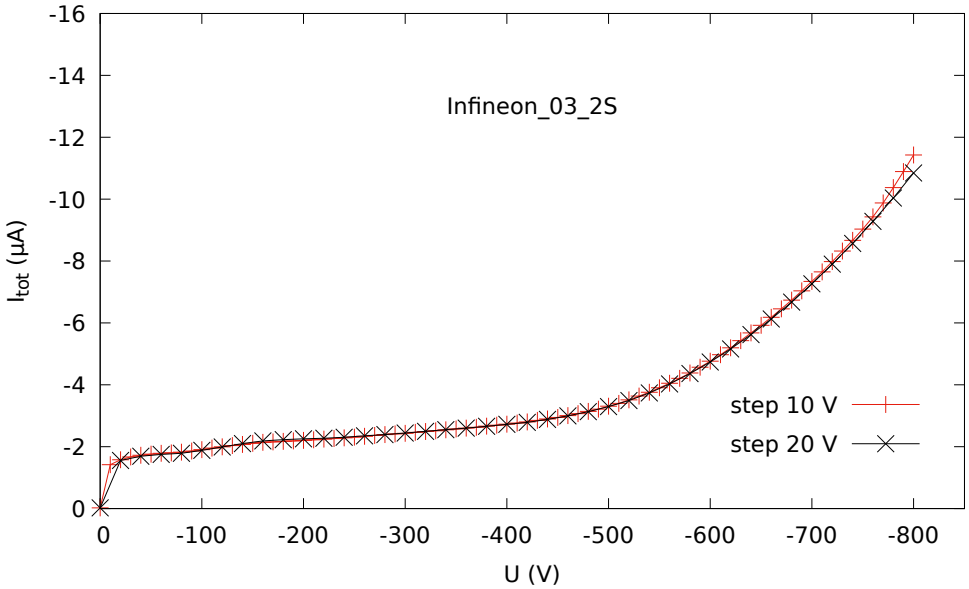
Infineon_03_2S
step 10 V
step 20 V
I_{tot} (µA)
U (V)
-16
-14
-12
-10
-8
-6
-4
-2
0
0
-100
-200
-300
-400
-500
-600
-700
-800

IV-Characteristics

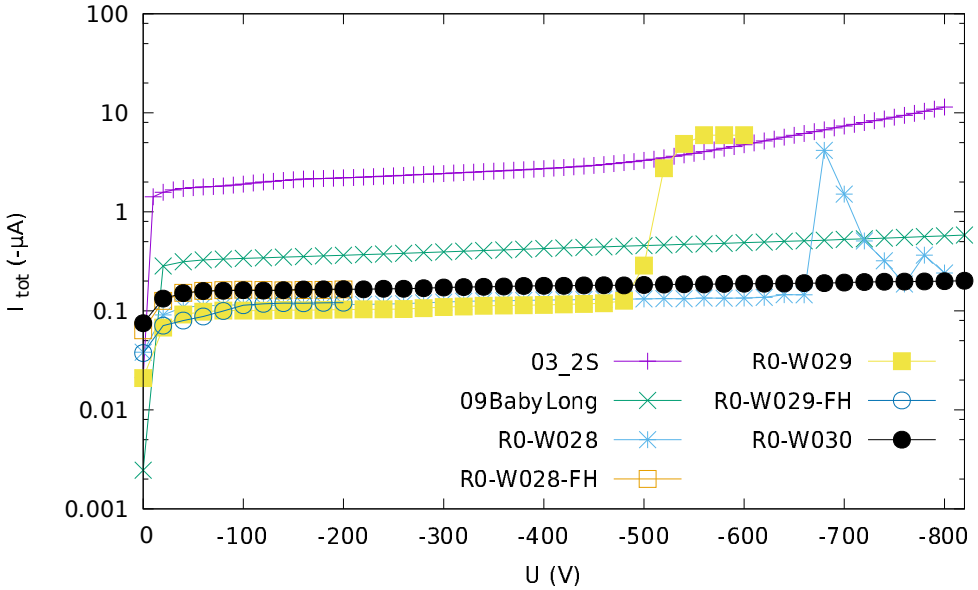

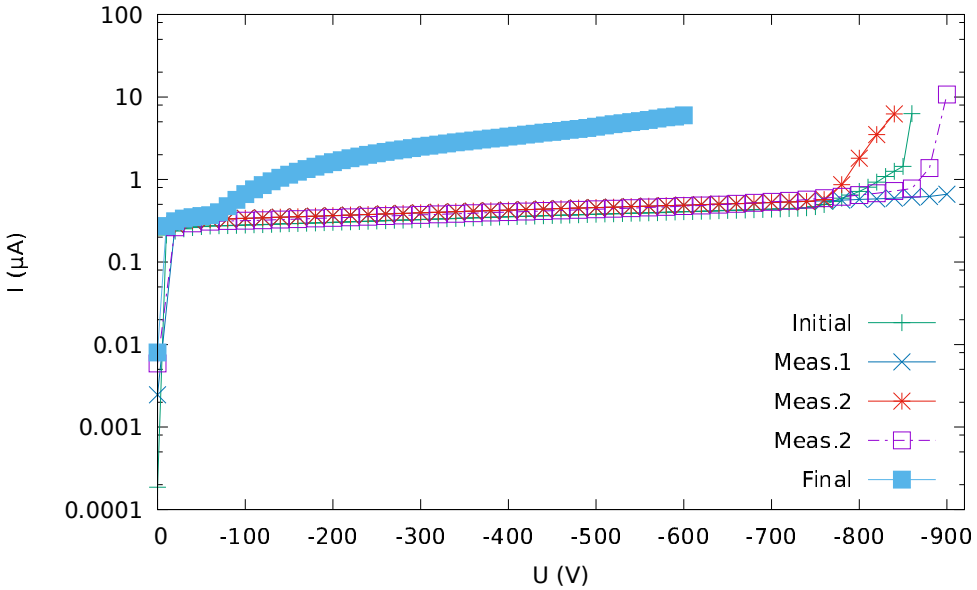

Humidity tests

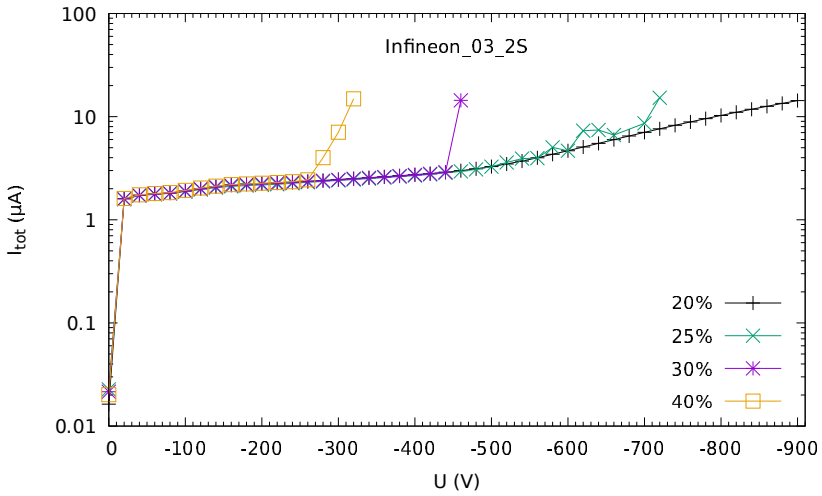

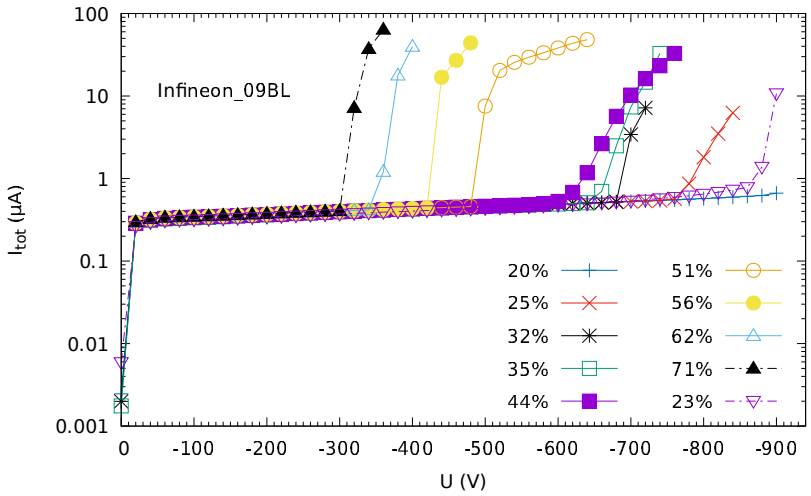

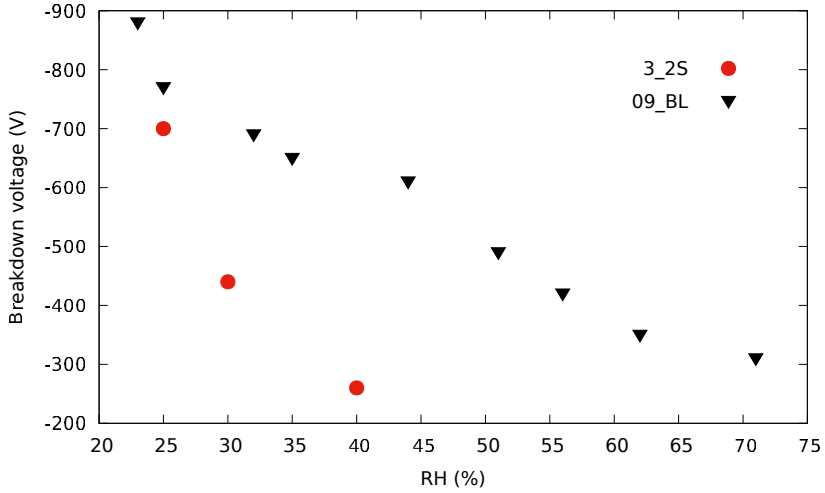

Coupling capacitance

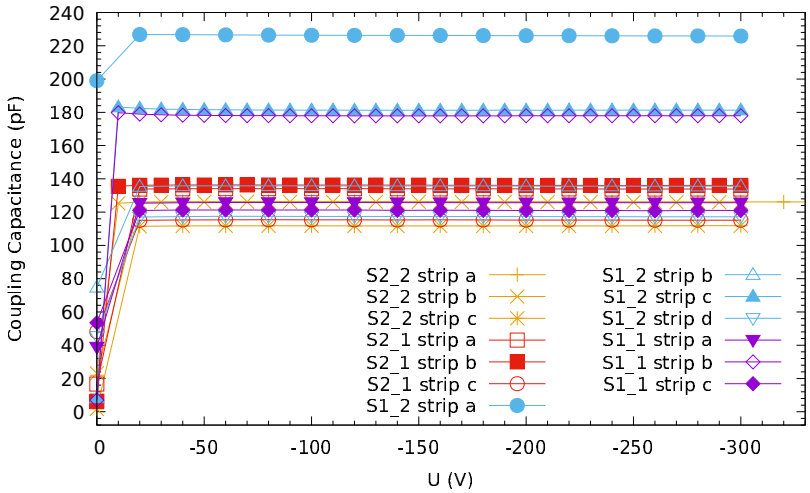

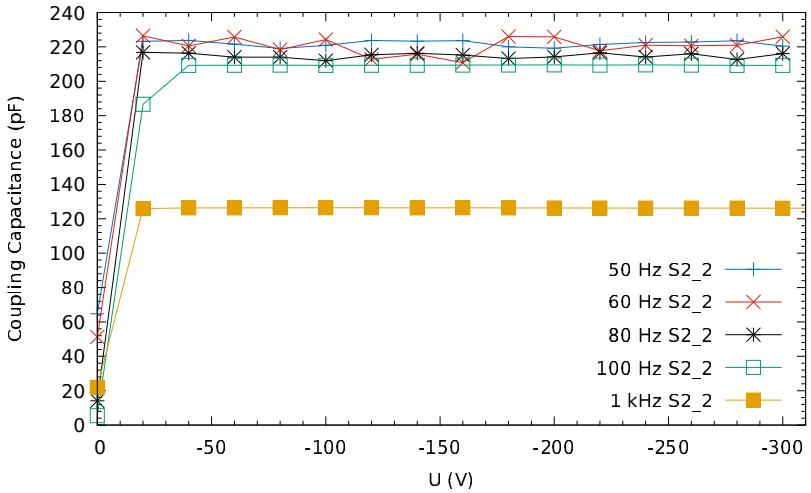

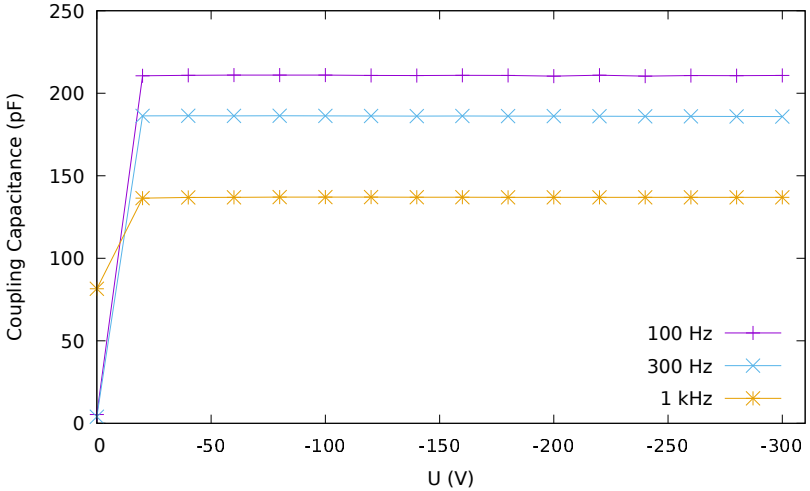

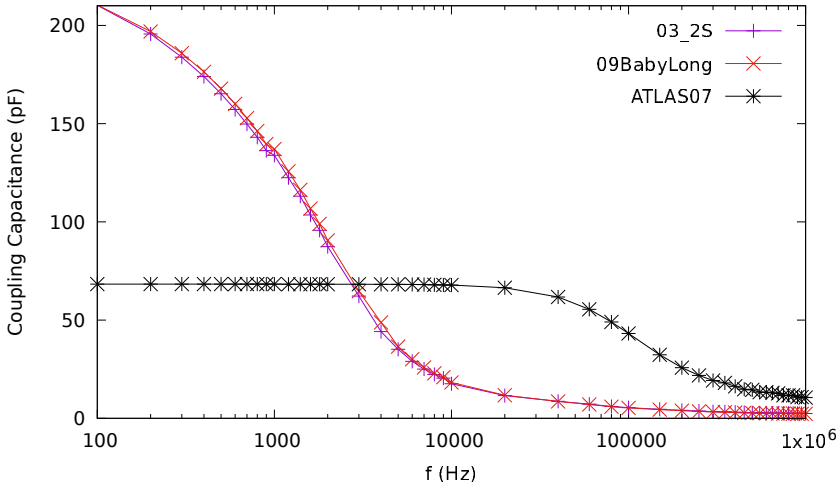

Full Depletion Voltage